1974-06

Modeling maneuvering airborne target motion with a coloring noise filter.

McKinley, David Howard

MODELING MANEUVERING AIRBORNE TARGET MOTION WITH A COLORING NOISE FILTER

David Howard McKinley

NAVAL POSTGRADUATE SCHOOL
Monterey, California

THESIS

MODELING MANEUVERING AIRBORNE TARGET MOTION
WITH A COLORING NOISE FILTER

by

David Howard McKinley

June 1974

Thesis Advisor: D. E. Kirk

UNCLASSIFIED

SECURITY CLASSIFICATION OF THIS PAGE (When Date Entered)

REPORT DOCUMENTATION PAGE		READ INSTRUCTIONS BEFORE COMPLETING FORM
1. REPORT NUMBER	2. GOVT ACCESSION NO.	3. RECIPIENT'S CATALOG NUMBER
4. TITLE (and Subtitle) Modeling Maneuvering Airborne Target Motion With a Coloring Noise Filter		5. TYPE OF REPORT & PERIOD COVERED Master's Thesis June 1974 6. PERFORMING ORG. REPORT NUMBER
7. AUTHOR(s) David Howard McKinley		8. CONTRACT OR GRANT NUMBER(s)
9. PERFORMING ORGANIZATION NAME AND ADDRESS Naval Postgraduate School Monterey, California 93940		10. PROGRAM ELEMENT, PROJECT, TASK AREA & WORK UNIT NUMBERS
11. CONTROLLING OFFICE NAME AND ADDRESS Naval Postgraduate School Monterey, California 93940		12. REPORT DATE June 1974 13. NUMBER OF PAGES 59
14. MONITORING AGENCY NAME & ADDRESS(if different from Controlling Office) Naval Postgraduate School Monterey, California 93940		15. SECURITY CLASS. (of this report) UNCLASSIFIED 15a. DECLASSIFICATION/DOWNGRADING SCHEDULE

16. DISTRIBUTION STATEMENT (of this Report)

Approved for public release; distribution unlimited.

17. DISTRIBUTION STATEMENT (of the abstract entered in Block 20, if different from Report)

18. SUPPLEMENTARY NOTES

19. KEY WORDS (Continue on reverse side if necessary and identify by block number)

Kalman Filtering
GFCS MK86

20. ABSTRACT (Continue on reverse side if necessary and identify by block number)

The method of modeling the motion of maneuvering airborne targets using a coloring filter having a white noise input is investigated. The characteristics of the simulated maneuvers depend on the time constant of the coloring filter and the standard deviation of the white noise input. The performance of a Kalman filter based on this model of target

DD FORM 1 JAN 73 1473 (Page 1)

EDITION OF 1 NOV 65 IS OBSOLETE
S/N 0102-014-6601

UNCLASSIFIED
SECURITY CLASSIFICATION OF THIS PAGE (When Date Entered)

Block #20 continued

motion compares favorably with the performance of filters derived from other models of target motion.

Modeling Maneuvering Airborne Target Motion With a Coloring Noise Filter

by

David Howard McKinley
Lieutenant Commander, United States Navy
B.A., University of Washington, 1964

Submitted in partial fulfillment of the
requirements for the degree of

MASTER OF SCIENCE IN ELECTRICAL ENGINEERING

from the

NAVAL POSTGRADUATE SCHOOL
June 1974

ABSTRACT

A method of modeling the motion of maneuvering airborne targets using a coloring filter having a white noise input is investigated. The characteristics of the simulated maneuvers depend on the time constant of the coloring filter and the standard deviation of the white noise input. The performance of a Kalman filter based on this model of target motion compares favorably with the performance of filters derived from other models of target motion.

TABLE OF CONTENTS

I. INTRODUCTION

A. GFCS MK 86

The Gun Fire Control System MK 86 Mod 3 (GFCS MK 86) is the U. S. Navy's first fully digital gun fire control system, so the system has been the subject of considerable study. Developed by the Lockheed Electronics Company, Inc. (LEC), a subsidiary of Lockheed Aircraft Corporation, the GFCS MK 86 is designed to track targets by digitally sampling target range, bearing, and elevation. The GFCS MK 86 is capable of controlling the 5"/54 MK 45 Mod 0 gun mount against surface, air, and both direct and indirect shore-fire targets.

B. GFCS MK 86 STUDY GROUP

Under the supervision of Professors Kirk, Titus, and Ward of the Electrical Engineering Department of the Naval Postgraduate School, the MK86 study group was formed in 1973. Based on the Operation and Test Evaluation Force Project C/S 79 report and as recommended by NSMSES, Port Hueneme, the effort of the study group was directed towards the anti-air mode of operation of the system. A FORTRAN simulation of the GFCS MK 86 was completed in June 1973 and reported in MSEE theses by U.S. Navy Lieutenants J. D. Gorman, T. J. Will, and D. R. Kidd, who simulated the Pre-filtering Data Processing, the Data Filtering, and Ballistics sections of the system, respectively. The radar

measurement noise statistics were estimated by L. S. Beers in September 1973. It is the purpose of this thesis to investigate the use of input forcing noise to simulate target motion in a constant-velocity model Kalman filter and to test the results obtained.

C. THE KALMAN FILTER

1. Discrete Equations

Difference equations can be used to describe the motion of an aircraft in the atmosphere, although in general one such equation is required for each of three coordinate axes. However, no set of deterministic equations can completely and accurately predict the precise influence that system modeling inaccuracies, air turbulence and mancuvers will have upon the aircraft's flight path. That is, aircraft motion is a stochastic process and must be discussed in probabilistic terms. Only linear difference equations will be used in this thesis since GFCS MK 86 has used a linear model to approximate target motion. Although nonlinear target motion undoubtedly occurs, it is beyond the scope of this thesis to investigate the validity of the approximations used. Rather, the purpose is to observe some of the results of filter operation.

2. Nomenclature

The discrete form of the model of target motion is

$$\underset{\sim}{x}(k+1) = \underset{\sim}{\Phi}(T)\underset{\sim}{x}(k) + \underset{\sim}{\Gamma}(T)\underset{\sim}{w}(k) + \underset{\sim}{\Delta}(T)\underset{\sim}{u}(k)$$

$$\underset{\sim}{z}(k) = \underset{\sim}{c}(T)\underset{\sim}{x}(k) + \underset{\sim}{v}(k).$$

A block diagram of these equations is shown in Figure 1.

The symbols used are defined as:

$\underset{\sim}{u}(k)$ is the m-dimensional vector of deterministic control inputs at time t = kT.

$\underset{\sim}{x}(k)$ is the n-dimensional state vector at time t = kT.

$\underset{\sim}{z}(k)$ is the q-dimensional vector of measured output at time k = kT.

$\underset{\sim}{v}(k)$ is the q-dimensional random measurement noise process at time t = kT.

$\underset{\sim}{w}(k)$ is the p-dimensional random input forcing noise process at time t = kT.

T is the sampling period.

k is a non-negative integer, the discrete time index.

$\underset{\sim}{\Gamma}$ is the nxp matrix which distributes the random input forcing noise $\underset{\sim}{w}(k)$.

$\underset{\sim}{\Delta}$ is the nxm matrix which distributes the control $\underset{\sim}{u}(k)$.

$\underset{\sim}{\Phi}$ is the nxm state transition matrix.

$\underset{\sim}{C}$ is the qxn output matrix.

The last four matrices are assumed to be time invariant, and are presumed to be known.

It was assumed that the measurement noise and input forcing noise processes have zero mean and are uncorrelated both with themselves and each other. In terms of the expected value operator E[f(k)] and Kronecker delta function δ_{kj},

$$E[\underset{\sim}{v}(k)] = E[\underset{\sim}{w}(k)] = \underset{\sim}{0} \text{ for all } k \geq 0$$

$$E[\underset{\sim}{v}(k)\underset{\sim}{v}^T(j)] = \underset{\sim}{Q}(k)\delta_{kj} \text{ for all } k,j \geq 0$$

$$E[\underset{\sim}{w}(k)\underset{\sim}{w}^T(j)] = \underset{\sim}{R}(k)\delta_{kj} \text{ for all } k,j \geq 0$$

The superscript T indicates matrix transposition.

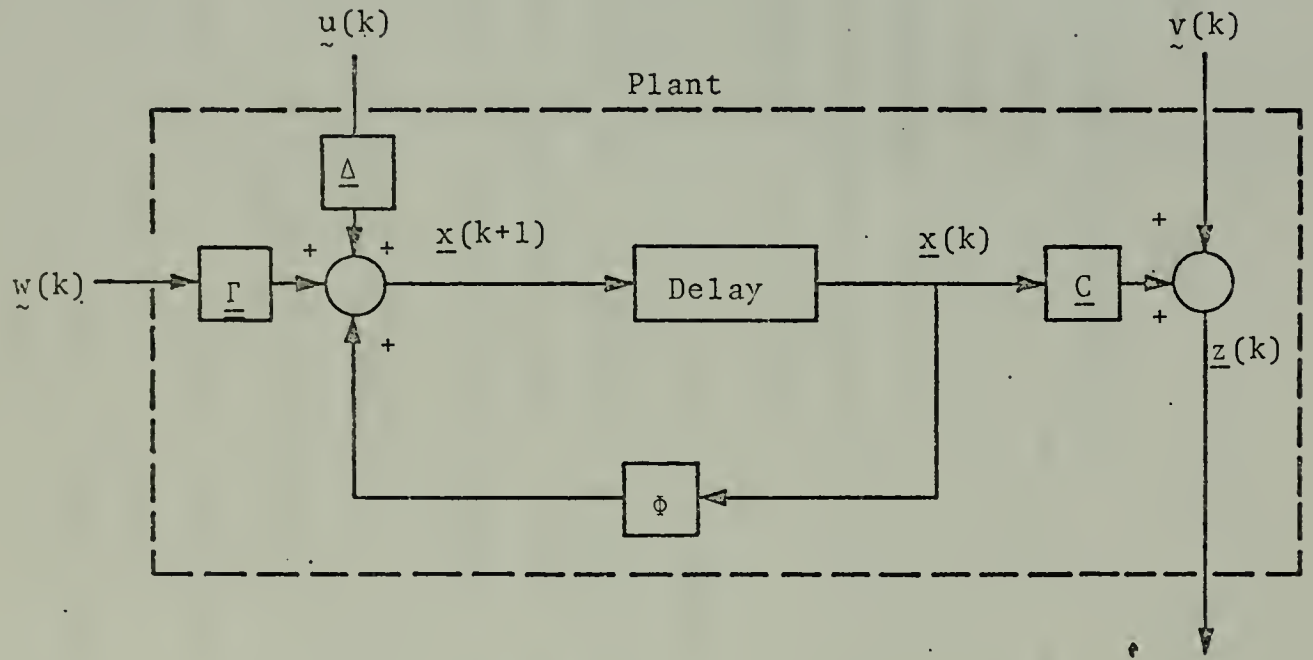

Figure 1. Block Diagram of Model for Discrete Target Motion.

The initial state is assumed to be a random variable with known mean and covariance and is uncorrelated with both the measurement noise and input forcing noise; that is

$$E[\underset{\sim}{x}(o)\underset{\sim}{v}^T(k)] = E[\underset{\sim}{x}(o)\underset{\sim}{w}^T(k)] = 0 \text{ for all } k \geq 0$$

and

$$E[\underset{\sim}{x}(o)] = \bar{\underset{\sim}{x}}_o, \; E\{[\underset{\sim}{x}(o) - \bar{\underset{\sim}{x}}_o][\underset{\sim}{x}(o) - \bar{\underset{\sim}{x}}_o]^T\} = P_o.$$

3. The Optimal Linear Estimator

An estimator (filter) is designed to estimate the state of the plant by using some optimization technique. When this technique is chosen to be the minimization of the trace of the covariance of estimation error matrix, and when the estimator is of the form

$$\hat{\underset{\sim}{x}}(k/k) = \hat{\underset{\sim}{x}}(k/k-1) + \underset{\sim}{G}(k)[\underset{\sim}{Z}(k) - \underset{\sim}{C}\hat{\underset{\sim}{x}}(k/k-1)],$$

then it has been shown in Reference 4 that the optimal linear estimator is the Kalman filter. In this equation the term in brackets is defined as the residual and

$\hat{\underset{\sim}{x}}(k/k)$ is the optimal estimate of $x(k)$ given measurements $\underset{\sim}{z}(o), \underset{\sim}{z}(1),\ldots,\underset{\sim}{z}(k)$,

$\hat{\underset{\sim}{x}}(k/k-1)$ is the optimal predicted value of $x(k)$ given measurements $\underset{\sim}{z}(o), \underset{\sim}{z}(1),\ldots,\underset{\sim}{z}(k-1)$.

These two quantities are related by the equation

$$\hat{\underset{\sim}{x}}(k/k-1) = \underset{\sim}{\Phi}\hat{\underset{\sim}{x}}(k-1/k-1) + \underset{\sim}{\Delta u}(k-1).$$

The optimal filter gains $\underset{\sim}{G}(k)$ are those gains which satisfy the following three equations:

$$\underset{\sim}{P}(k/k-1) = \underset{\sim}{\Phi P}(k-1/k-1)\underset{\sim}{\Phi}^T + Q(k-1)$$

$$\underset{\sim}{P}(k/k) = \underset{\sim}{P}(k/k-1) - \underset{\sim}{G}(k)\,\underset{\sim}{C P}(k/k-1)$$

$$\underset{\sim}{G}(k) = \underset{\sim}{P}(k/k-1)\ \underset{\sim}{C}^{T}\ [\underset{\sim}{C}\ \underset{\sim}{P}(k/k-1)\underset{\sim}{C}^{T} + R(k)]^{-1}$$

The covariance of estimation error matrix $\underset{\sim}{P}(k/k)$ and the covariance of one-step prediction error matrix, $\underset{\sim}{P}(k/k-1)$ are defined as

$$\underset{\sim}{P}(k/k) = E\{[\hat{\underset{\sim}{x}}(k/k) - \underset{\sim}{x}(k)][\hat{\underset{\sim}{x}}(k/k) - \underset{\sim}{x}(k)]^{T}\}$$

$$\underset{\sim}{P}(k/k-1) = E\{[\hat{\underset{\sim}{x}}(k/k-1) - \underset{\sim}{x}(k)][\hat{\underset{\sim}{x}}(k/k-1) - \underset{\sim}{x}(k)]^{T}\}$$

D. INPUT FORCING NOISE

1. Effect on Gain Calculations

The filter will tend to weight early measurements rather heavily, since in the absence of other data each new measurement must be considered a good estimate of target location. After several measurements have been made on a non-maneuvering target, however, the size of the residual and the magnitude of the gains will tend to be reduced. Each new measurement will now be weighted more lightly since the filter is relatively confident of the target's location. After G(k) has approached some value G, the filter is then in the steady state. The gain schedule in steady state is such that the effect one or two poor measurements has on filter performance tends to be rather small, thus providing a certain amount of measurement noise immunity while tracking a target. On the other hand, since the steady-state Kalman filter tends to be relatively insensitive to change, it may require several measurements before it recognizes a significant target maneuver.

Note that since the optimal filter gains are dependent upon the covariance of prediction error matrix, the gains are therefore dependent upon the $\underset{\sim}{Q}$ matrix. Within limits, then, the forcing noise matrix $\underset{\sim}{Q}$ can be used to "open up" the gain schedule so that new measurements will be given reasonable weight to allow the filter to track maneuvering targets accurately and yet provide smooth tracking during steady state conditions.

2. GFCS MK 86 Application

The GFCS MK86 utilizes a Kalman filter for its estimation and prediction technique. The filtering is done in rectangular coordinates. The motion of the target in each of the three coordinate axes is assumed to be uncoupled; that is, motion in one direction does not interact with motion in either of the other two directions. The filter also operated in either the constant-velocity or constant-acceleration mode. In the constant-velocity mode target accelerations are assumed zero. For target accelerations in excess of 0.1 meters/sec^2, the filter adaptively switches to the constant-acceleration mode. In this mode target acceleration is calculated up to a maximum of 50 meters/sec^2 (5 g's); accelerations greater than this are set to this maximum value.

In each of these modes, the filter gain schedule was derived under the assumption that $\underset{\sim}{Q}$ is zero. This is not realistic since input forcing noise must exit in a physical situation due to air turbulence, maneuvering, and

modeling inaccuracies. An appropriate value for $\underset{\sim}{Q}$, however, could allow the filter to operate in the constant-velocity mode and still accurately estimate accelerated target motion.

3. Input Forcing Noise

When used in conjunction with a constant-velocity model, the assumption that the forcing noise $\underset{\sim}{w}(k)$ is white corresponds physically to an aircraft moving at a constant velocity and experiencing only such random acceleration disturbances as small-scale air turbulence. However, during a sustained maneuver such as a turn or a dive, or in large-scale turbulence, the random forcing acceleration will be correlated over several sampling periods. One method for obtaining correlated noise is to pass white noise through an appropriate "coloring" filter as shown in Figure 2 and as reported in Reference 3.

It is the purpose of this thesis to improve the Kalman filter's performance by improving the model of the system. The system investigated is that of a maneuvering airborne target and a coloring noise filter is used to model this motion. The coloring filter is designed to correlate the white input forcing noise in such a way that the accelerations experienced during an aircraft maneuver are proportional to the standard deviation of the forcing noise. The coloring filter is implemented by augmenting the state transition ($\underset{\sim}{\Phi}$) matrix of a constant-velocity model of the Kalman filter, and its performance compared with four other filters.

Figure 2. Block Diagram of Coloring Noise Filter.

II. THE COLORING FILTER

A. THEORETICAL BASIS

1. Filter Transfer Function

One form a coloring filter can take is that of a low pass filter with white noise as the input and colored or correlated noise as the output. One low pass filter has an s-domain representation of the form

$$H(s) = \frac{Y(s)}{W(s)} = \frac{\alpha}{s + \alpha} ,$$

where W(s) is the input white noise, Y(s) is the correlated output, and H(s) is the filter transfer function. The time domain impulse response of the transfer function is $h(t) = \alpha e^{-\alpha t}$, a decaying exponential whose magnitude depends upon the time t and the constant α. With a specific discrete sampling time, say $t = T$, α can then be varied to obtain different exponential decay rates and thereby select the amount of correlation between successive samples. This is accomplished by looking at the relative magnitude of the product αT; the smaller the product for αT, the less the magnitude of the preceeding sample will have decayed before the next sample is taken and the more correlation there is between successive samples. The forcing noise is approximately white when the product αT is large enough so that $e^{-\alpha T}$ is close to zero before the next sample is taken so that the successive samples are essentially uncorrelated.

2. Time Domain Analysis

A time domain analysis of the coloring filter results in the continuous differential equation

$$\dot{y}(t) = - \alpha y(t) + \alpha w(t).$$

If w is piecewise constant, then the state variable representation for this equation is

$$y(k+1) = \Phi y(k) + \Delta w(k)$$

where

$$\Phi = e^{-\alpha T}, \quad \Delta = 1 - \Phi = 1 - e^{-\alpha T}.$$

Using the Taylor series expansion for the exponential function, both Φ and Δ can then be approximated as $\Phi = 1 - \alpha T$ and $\Delta = \alpha T$, so long as αT is small when compared to 1.

B. TARGET MANEUVER SIMULATION

Target tracks were available on magnetic tape from test runs of the GFCS MK86 (see Section III), although significant target maneuvers appear in elevation only. In order to make subsequent track comparison more meaningful, the discrete simulation measurement time was selected to be T = 0.25 seconds, the same as the GFCS MK86 radar sampling time, and the coloring filter simulation was restricted to maneuvers in the Z direction only. Although acceleration values were calculated using data obtained from such a one-dimensional track, it is reasonable to extend the results to both the X- and Y-directions since motion in each coordinate axis of the GFCS MK86 is assumed uncoupled.

1. Subroutine Color

Equation (1) was implemented in FORTRAN with subroutine COLOR acting as the coloring filter. Subroutine COLOR first generates statistically independent Gaussian random numbers to represent the white forcing noise w(k) by calling subroutine GAUSS. Each random number thus obtained is an input to the coloring filter and the outputs are correlated noise. Each colored forcing noise sample represents an acceleration and is used to update a simulated one-dimensional target track in elevation by integrating the equations

$$\dot{x}_1 = x_2$$

$$\dot{x}_2 = x_3$$

$$\dot{x}_3 = - \alpha x_3 + \alpha w$$

where α is a coloring filter parameter and w is piecewise constant.

2. Starting Number

Several tracks were simulated and plotted on the CALCOMP plotter. It immediately became apparent that the tracks generated by the coloring filter were highly dependent upon the starting number used to call subroutine GAUSS. It was decided that proper track analyzation would require a minimum target maneuver of 15 seconds duration, so a useful starting number was defined as a number which was able to sustain a single simulated maneuver for at least 15 seconds. Two sample starting numbers which did not meet this criterion

generated tracks shown in Figures 3 and 4. It should be noted that the steepness of the tracks appears to be about the same; only the maneuver's duration is different. Several simulations were also conducted using a satisfactory starting number and varying the standard deviation of the input white forcing noise.

3. Acceleration Calculation

The simulations thus obtained were then piecewise approximated by straight line segments drawn through no less than four points. The slope of each line represents the average target velocity for at least one second of time. The maneuver was considered terminated when the slope of the velocity line became constant. The average acceleration for the maneuver was then calculated by plotting the slope of the position line segments against time.

A linear relationship was found to exist between the standard deviation of the input forcing noise and the accelerations attained during the simulated dive, in that an increase of about .61 ft/sec^2 (.019 g's) in acceleration was obtained for each 1.0 increase in white noise standard deviation. This relationship was used to generate tracks with the accelerated motion desired. Because an acceleration of about 16 ft/sec^2 (0.5 g's) was experienced during an actual GFCS MK86 test run, it was of special interest for comparison purposes to find the standard deviation required to generate a maneuver of this type. A standard deviation of 26.0 generated the simulated track, shown in Figure 5. The

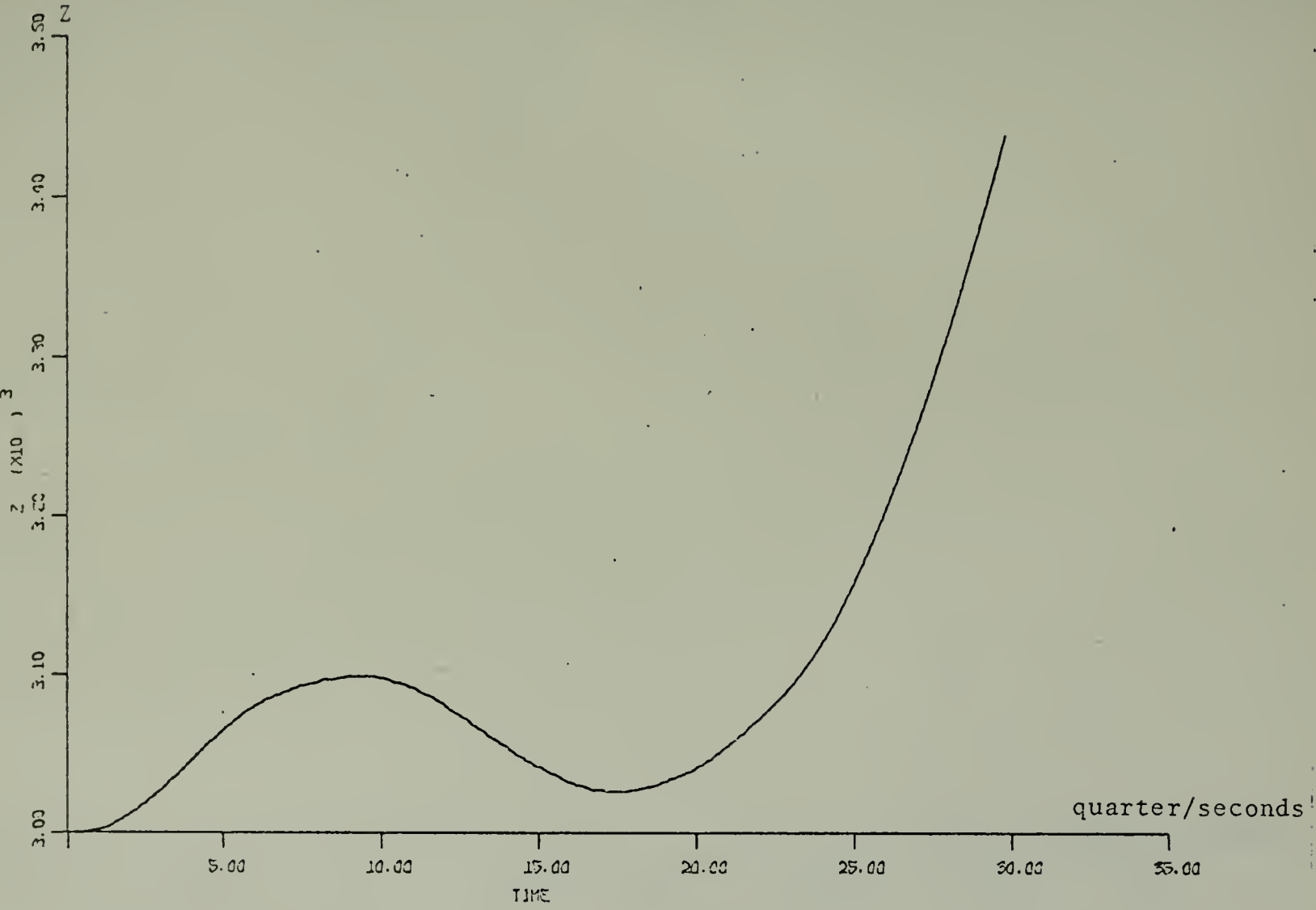

Figure 3. Simulated Target Track.
(Starting number = 511761937)

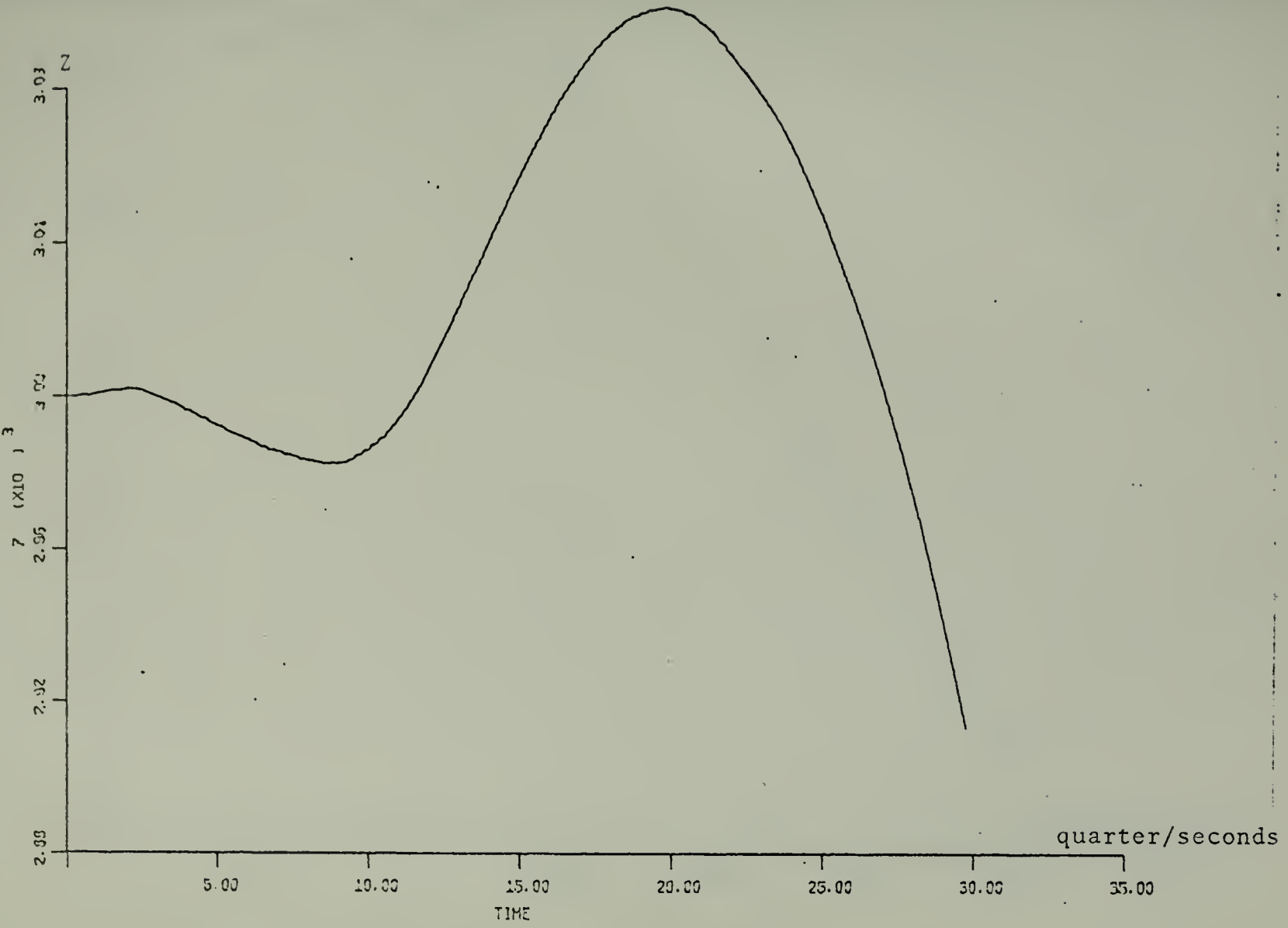

Figure 4. Simulated Target Track.
(Starting numer = 696981987)

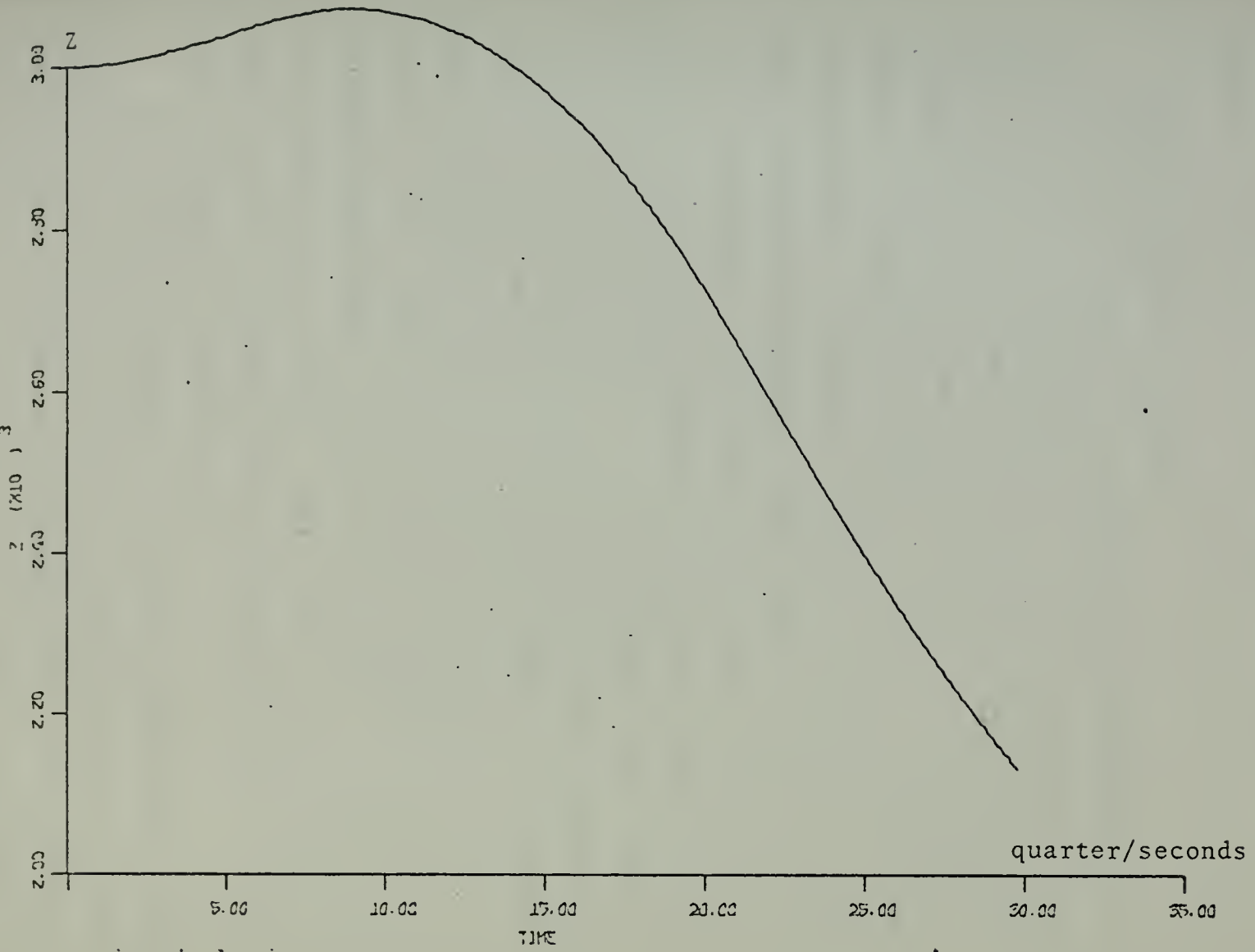

Figure 5. Simulated Target Track.

acceleration simulated during this maneuver is shown in Figure 6.

C. COLORING FILTER STATISTICS

The mean, variance, and probability distribution of the output of the coloring filter were also of interest. Filter means and variances were calculated for several white noise standard deviations from a time average of 10,000 points and are as indicated in Table I. No significant difference was noted when the transient response, defined to be the first 100 numbers generated, were ignored for the statistical calculations. If the input to a linear filter is Gaussian, it is well known that the filter output will be Gaussian as well. As a test for the statistics of the colored noise output, a scatter diagram of the random acceleration values was plotted for 6000 numbers. Of these 6000 numbers generated, only 288 (4.8%) were outside the 2σ region. This result is in excellent agreement with the Gaussian probability of 4.5% of the points as theoretically being outside this region. These three statistical measurements seemed to indicate that the coloring filter was reasonably well-behaved statistically.

It is shown in Appendix A that the steady state standard deviation of the colored noise is some fraction of the white noise standard deviation. The magnitude of this fraction as well as the values for Φ and Δ depend upon the values chosen for the sampling time T and the correlation factor α. T was

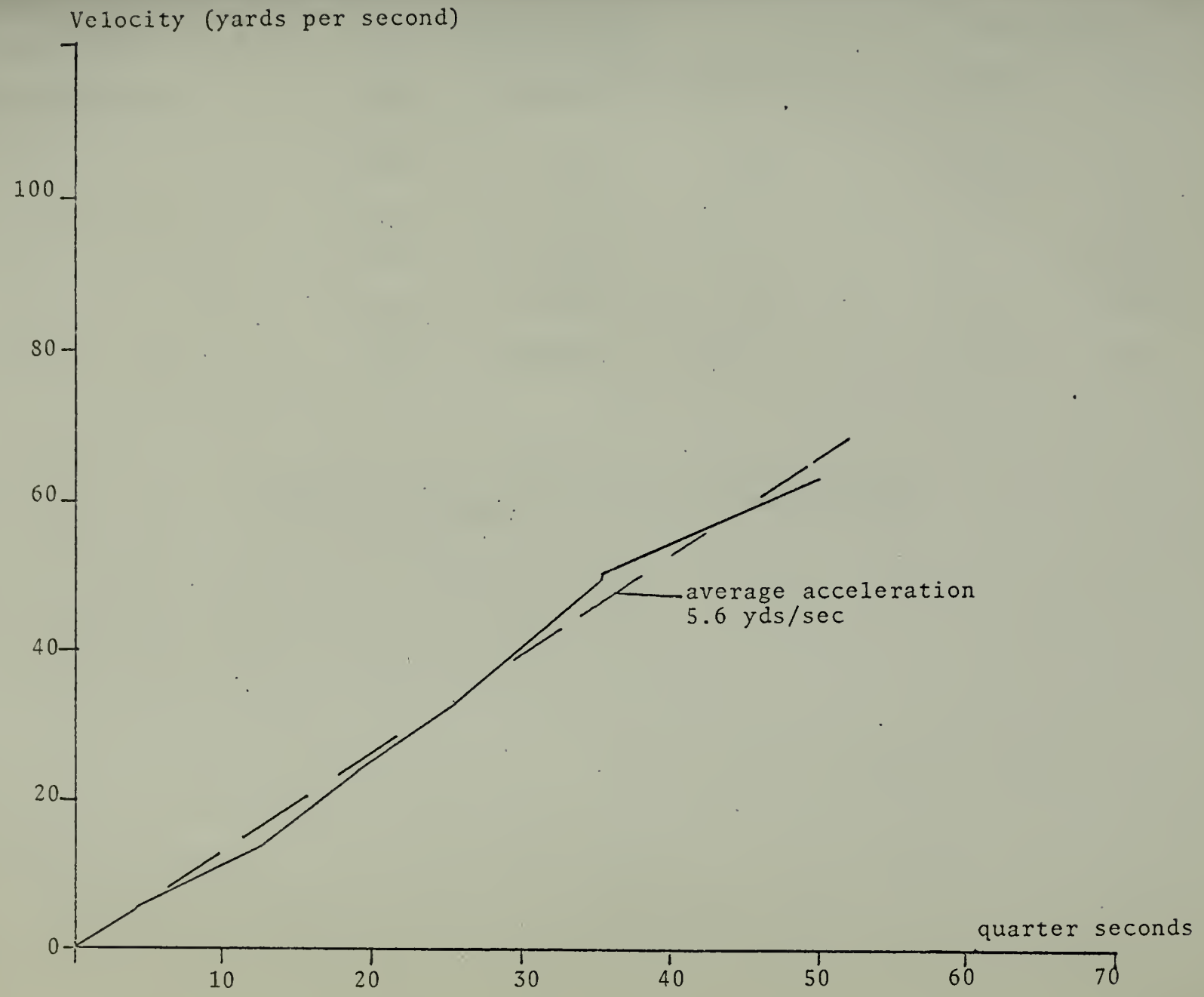

Figure 6. Simulated Track Acceleration.

White Noise	Colored Noise			Acceleration	
Standard Deviation	Mean	Variance	SD	Ft/Sec	g's
2.0	0.0317	0.102	0.032	1.15	0.036
15.0	0.232	5.735	2.4	9.0	0.28
26.0	0.403	17.218	4.15	16.1	0.50
50.0	0.774	63.718	7.99	32.4	1.005
85.0	1.315	184.010	13.6	51.6	1.6

Table I.

Statistical Properties of the Coloring Filter.

chosen as 0.25 seconds, the radar sampling time of the GFCS MK86. The low pass filter time constant must be long when compared to the sampling time in order for succeeding samples to be correlated, so that a filter time constant of 5 seconds was selected. After substituting these values into Equation (1) of Appendix A, the theoretical standard deviation of the resulting colored noise was shown to be 16% of the standard deviation of the white input forcing noise. As a check on the validity of the results obtained, the standard deviations of the tracks generated by the coloring filter were compared to the theoretical values predicted in Appendix A. In every case the difference between the actual and theoretical values for standard deviation was less than 1%.

D. AUGMENTED STATE TRANSITION MATRIX

The coloring filter is implemented in the Kalman filter in the form of an augmented state transition matrix of third-order model of constant acceleration aircraft motion. The block diagram of this model is shown in Figure 7. The equation for acceleration in the constant-acceleration model for target motion is

$$x_3(k+1) = x_3(k)$$

where $x_3(k)$ is the acceleration and T is the sampling time. In the coloring filter model, however, this equation becomes

$$x_3(k+1) = c_1 x_3(k) + c_2 w_1(k)$$

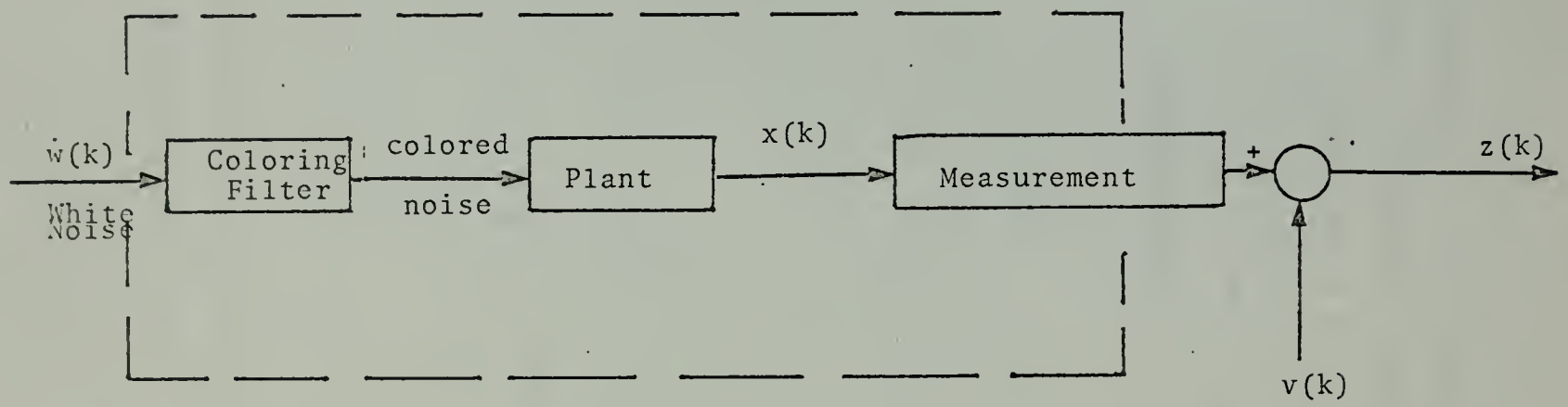

Filter 7. Block Diagram of Augmented Plant Model with Colored Filter.

where c_1 and c_2 are constants determined by the sampling time T and the filter parameter α. The solution to this latter equation is, of course, the same as that for the coloring noise filter, so that c_1 is the Φ of the coloring noise filter solution ($\Phi = e^{-\alpha T}$) and c_2 is the Δ of the coloring noise filter ($\Delta = 1 - \Phi = 1 - e^{-\alpha T}$). Using $T = 0.25$, $\alpha = 0.2$ for the reasons already indicated, the augmented acceleration model is then

$$x_3(k+1) = .9512x_3(k) + .0488w_1(k).$$

The state transition matrix Φ and the forcing noise weighting matrix $\underset{\sim}{\Gamma}$ for this augmented third order model may now be calculated by classical means. The general one-dimensional form of these two matrices is

$$x_1(k+1) = x_1(k) + Tx_2(k) + [\frac{T}{\alpha} - \frac{1}{\alpha^2}(1-e^{-\alpha T})]x_3(k)$$
$$[\frac{T^2}{2} - \frac{T}{\alpha} + \frac{1}{\alpha^2}(1 - e^{-\alpha T})]\, w(k).$$

$$x_2(k+1) = x_2(k) + \frac{1}{\alpha}(1 - e^{-\alpha T})\, x_3(k)$$
$$+ [\, T - \frac{1}{\alpha}(1 - e^{-\alpha T})]\, w(k).$$

$$x_3(k+1) = e^{-\alpha T}\, x_3(k) + (1 - e^{-\alpha T})\, w(k).$$

The specific values for the above equations with the aforementioned filter characteristics are

$$x_1(k+1) = x_1(k) + 0.25x_2(k) + 0.30x_3(k) + 0.00175w(k)$$
$$x_2(k+1) = x_2(k) + 0.244x_3(k) + 0.0060w(k)$$
$$x_3(k+1) = 0.9512x_3(k) + 0.0488\, w(k).$$

III. FILTER TESTING

A. FILTER TESTING PROGRAM

It has been shown in this thesis that aircraft maneuvers can be simulated by coloring the white input forcing noise w(k) and that the acceleration experienced during the maneuver is proportional to the standard deviation of w(k). It remains to show how the coloring filter performs in comparison with other filters while tracking the same target.

1. Monte Carlo Simulation Program

Filter testing was performed using the Monte Carlo Simulation Program (MCSP) as developed and reported on by Ketron [Ref. 2]. MCSP is a general program which computes statistics concerning the response of a filter to noisy measurements of a deterministic input target track. It has the capacity to accept as many as 233 three-dimensional track points and, when suitably modified, can be operated completely uncoupled in one dimension.

2. One-Dimensional Track

Four reasons required that the filter testing be performed in the elevation dimension only. First, movement in each axis had already been assumed uncoupled. To ensure that this was actually the case, the MCSP required that X and Y position information be set to zero so that no motion existed which could be coupled into elevation. Second, the derivation of the coloring filter equations and its subsequent

track simulation was performed in one dimension; it would seem that valid testing should also be done in one dimension. Third, as will be covered in the next section, the GFCS MK86 tracks available had significant maneuvers in elevation only. Since these tracks were used as the deterministic input to the filter testing program, the filter could best be tested in one dimension only. Finally, results from motion in one dimension are easier to analyze than those obtained from simultaneous motion in three dimensions.

B. TRACK INPUT

1. GFCS MK86 Data

An actual aircraft target track was used as the deterministic input to the MCSP for filter testing and comparison. Such tracks were readily available from the initial test and evaluation of the GFCS MK86 conducted in August and September 1972 aboard USS Norton Sound (AVM-1) in the Southern California operating areas. Four different types of aircraft targets were used for test runs: an S-2F towed sleeve, an A-4 jet aircraft, a towed drone unit, and a self-propelled BQM drone. Weather conditions for the tests were ideal with sunny skies, clear visibility, and calm seas. The ship maintained a steady course at 5 knots during all aircraft runs.

A large amount of data was recorded and preserved on magnetic tape for post-test analyzation. For this thesis, the only target data of interest was target X, Y, and Z

inertial position after transformation from spherical coordinates. This data was recorded at the radar sampling rate of 4 Hertz and was recovered for evaluation at NPS by transferring the data from magnetic tape to the data cell via disc storage. Desired data was then retrieved from the data cell through subroutine FETCH.

2. Data Limitations

The paucity of truly maneuverable target test runs available caused a significant analyzation problem. The data from many target runs had been examined before any were found in which accelerated maneuvers occurred; indeed, almost every test run was of constant velocity, unchanging elevation, and straight line trajectory. Notable exceptions to this were the maneuvering runs performed by a BQM drone on 1 September 1972. In these runs the drone started from a range of about 18,000 yards from the ship at an elevation of about 3,200 yards. After several seconds of level flight at a constant velocity, however, the drone performed a relatively constant acceleration dive of about 30 seconds duration while maintaining a relatively straight course towards the target ship. The velocity and acceleration experienced during the runs were calculated using the same analyzation techniques as outlined for the coloring filter (see Section II.)

3. Maneuver Characteristics

The largest acceleration experienced in a dive on these tracks was about 16 ft/sec^2 (½ g); it was the last 233

points of this track which were used at the input to MCSP. During this portion of the track the aircraft exhibited a very slight but continuous climb in elevation until point 128 was reached, about 32 seconds after the start of the test program data. At this point the aircraft commenced the constant-acceleration dive, which continued for the rest of the track. The position, velocity, and acceleration plots of this track are shown in Figures 8, 9 and 10, respectively. It should be noted that the track plotted already had been converted from spherical to Cartesian coordinates and therefore consists of noisy data.

C. FILTER TEST AND RESULTS

1. The Performance Criterion

Three quantities were used to judge the relative effectiveness of each of the filters: filter position estimation error, filter estimated position, and filter estimated velocity. The purpose of these three particular criteria is to ascertain which of the filters provides accurate, smooth, and timely target position and velocity information as outputs.

Filter position estimation error is an important quantity for evaluating filter effectiveness since it indicates how close filter position estimate is to actual target position. Since the two latter quantities are available from the filter, the position estimation error can be computed for each point along the track. The mean of the

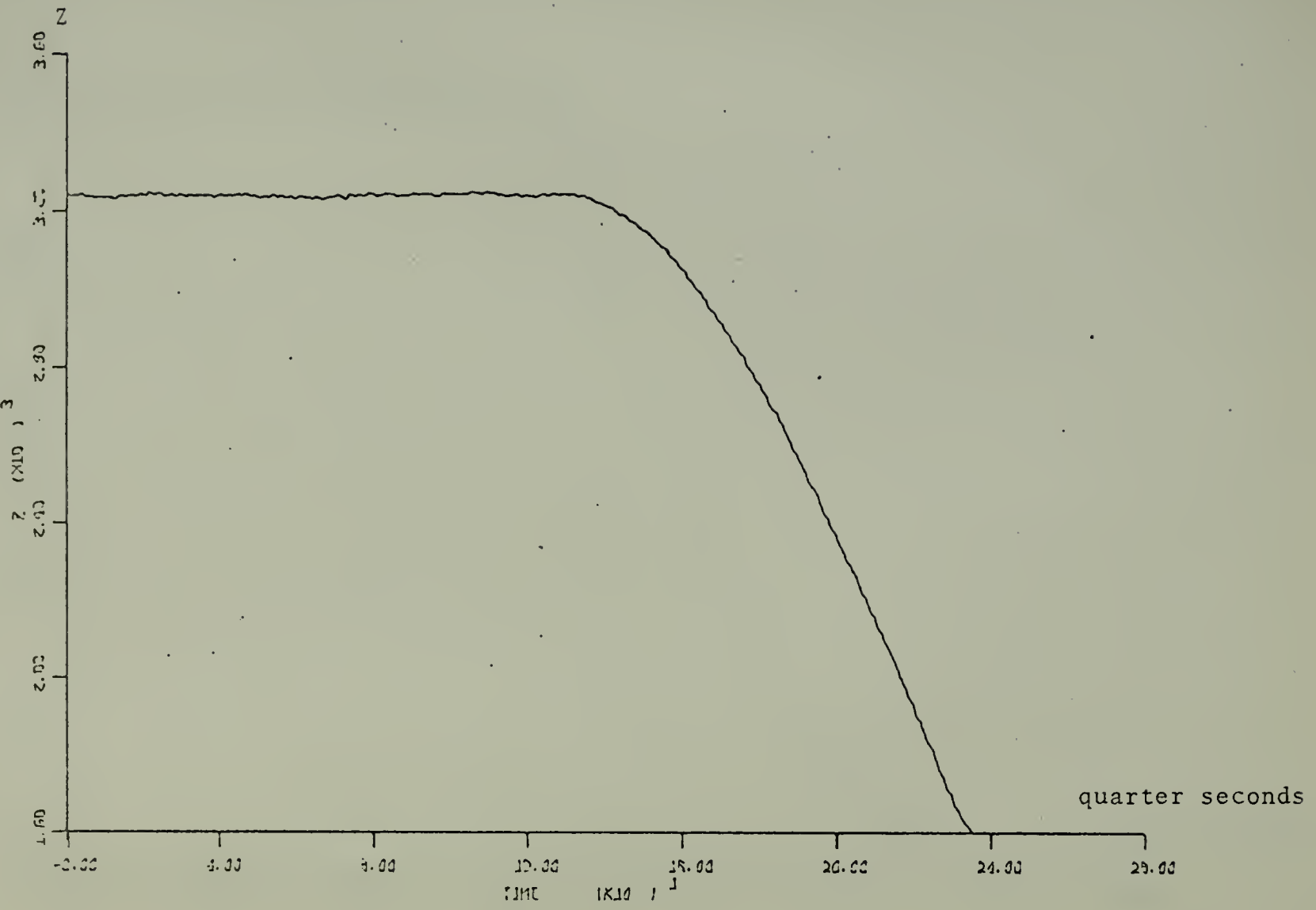

Figure 8. GFCS MK86 Track

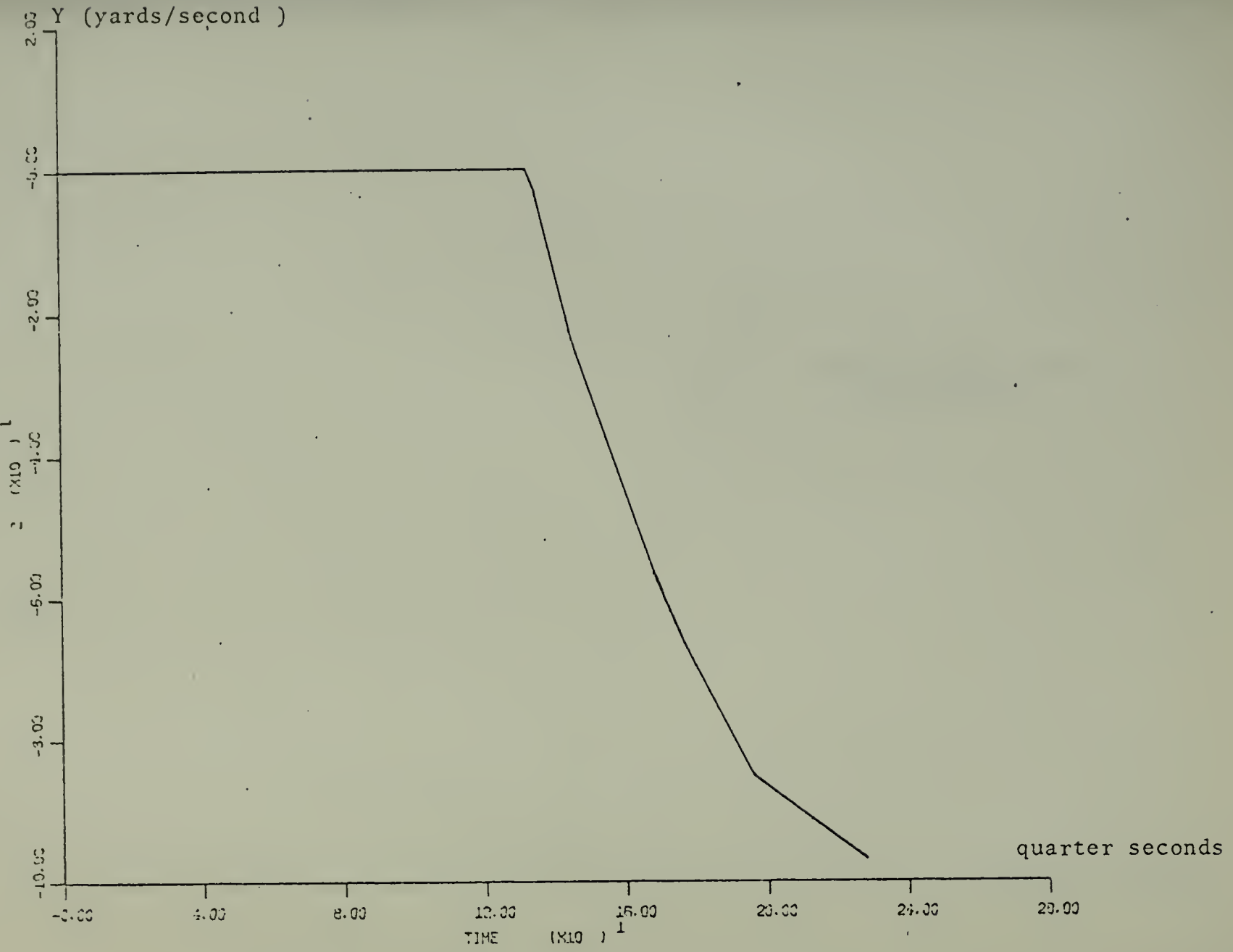

Figure 9. GFCS MK 86 Track Average Velocity.

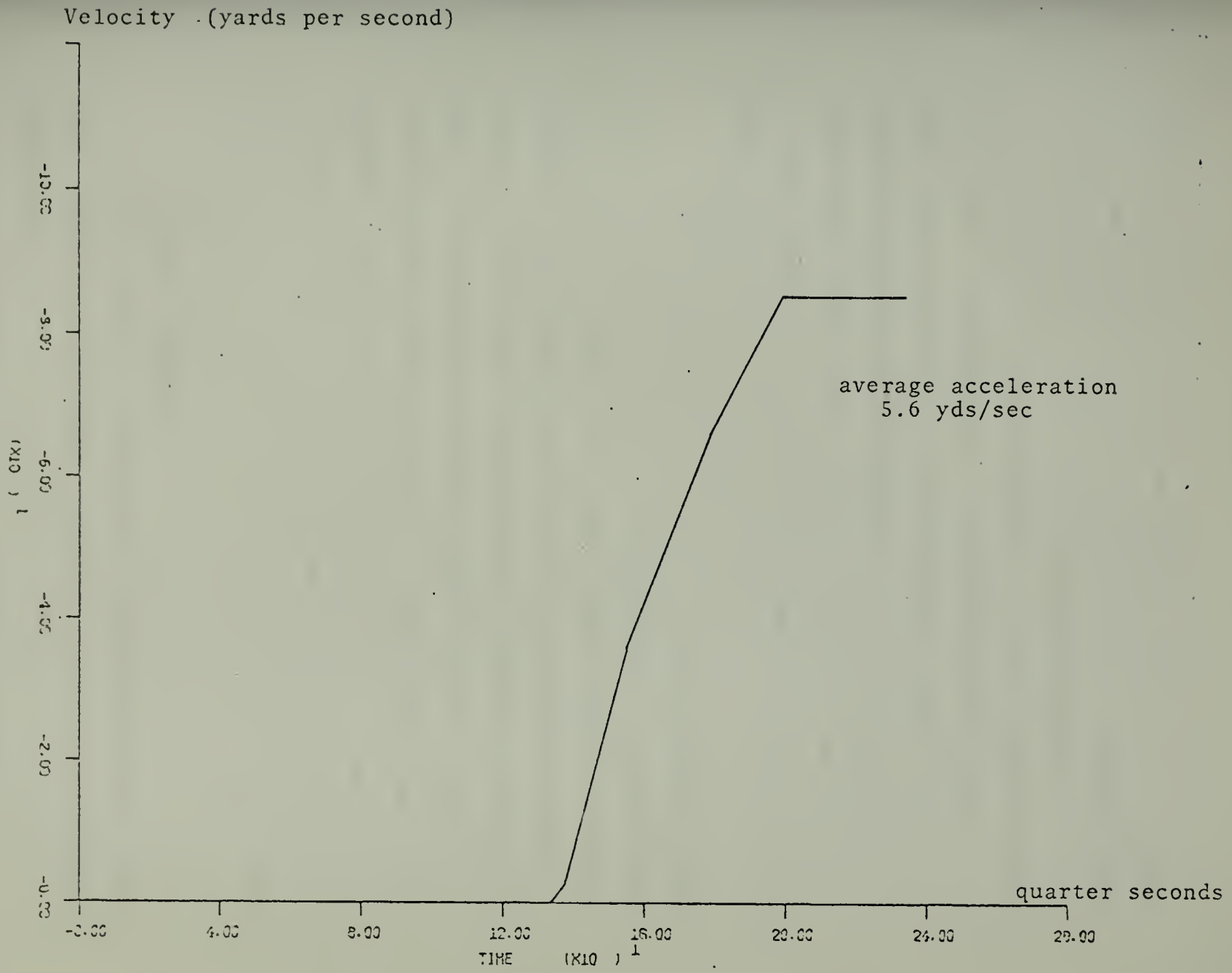

Figure 10. GFCS MK86 Track Acceleration.

magnitude of the position estimation errors for the entire track can then be calculated and used as an average figure of merit for the filter's performance during the run.

Filter estimated position is also a useful indicator of a filter's performance. A graph of filter position estimates versus time can be matched against that of the deterministic input track and compated for tracking quality. A filter which lags behind during a maneuver or which tends to see a maneuver where none exists may not provide information accurate enough for many purposes.

The ability of the filter to estimate velocity must also be examined. Velocity estimates have an enormous effect on the accuracy of gun orders since the fire control computer must predict the position of the target several seconds in the future based upon the information now available. An inaccurate velocity estimate could obviously cause large gun order errors and lead to rather disastrous consequences. A plot of velocity estimates versus time can then be compared to that of the approximate velocity of the actual track and can then be used to judge the filter's performance in this critical area.

2. Filter Comparison

For comparison purposes, a filter was derived and tested against the GFCS MK86 track for each of the following plant models:

1) Constant-velocity ($1/s^2$) model with $Q = E[w(k)w(k)^T] = 1.0$

2) Constant-velocity model with Q =676.0

3) Constant-acceleration ($1/s^3$) model with Q = 1.0

4) Constant-acceleration model with Q = 67.0

5) Constant-velocity model with augmented state transition matrix (coloring filter) with Q = 676.0.

In each case the measurement noise standard deviation was assumed to be a constant of 5.0 yards.

a. Constant-Velocity Model with Small Q

The constant-velocity plant model with zero Q is one of the simplest models which can be used for non-maneuvering target motion. The small, non-zero value for Q used in this filter's testing was selected so that the on-line gain calculation used in MCSP would reach steady state without requiring truncation at some arbitrary number of iterations as would be required for a Q of zero. The gain schedule reaches a small steady state value after a short time and thereafter becomes relatively insensitive to a change in target motion, such as would occur during a dive.

It was therefore expected that this filter would provide accurate estimates during the constant-velocity portion of the input track but fairly inaccurate estimates during the accelerated motion portion of the track. When the target reverts to a relatively constant velocity, however, the filter should slowly settle down and begin to estimate target position accurately once again. The mean position estimation error for this run should be fairly large, however, because of the input track's maneuvering.

Some of these expectations were indeed observed from the test results, which are illustrated in Figures 11 and 12. The filter generated estimated position errors of up to 30 yards when the aircraft first entered the dive; following this the velocity estimates tended to be rather poor, showing an eight yard/sec lag towards the end of the dive. Estimation of both position and velocity were quite accurate up to the aircraft dive point, as expected.

b. Constant Velocity Model with Large Q

The constant-velocity plant model with a large Q is designed to keep the filter gains fairly high so that the filter will be able to follow accelerated target motion when it occurs. The tendency for a filter with large gains is to accept each new measurement as if it were a valid indication of target position and to rely less heavily on past measurements. The trick is to find Q so that the gains are large enough to handle the most radical maneuver expected, yet small enough so that smooth tracking results during the constant-velocity phases of target motion. In the absence of other information and since the track was known beforehand to contain a ½ g maneuver, the Q which generated a ½ g dive when used with the coloring filter was selected.

It was expected that the relatively large gains would enable the filter to provide accurate position and velocity estimates during the entire track. The estimates were expected to be less consistent during the constant-velocity portion of the track than those of the constant-velocity model with a

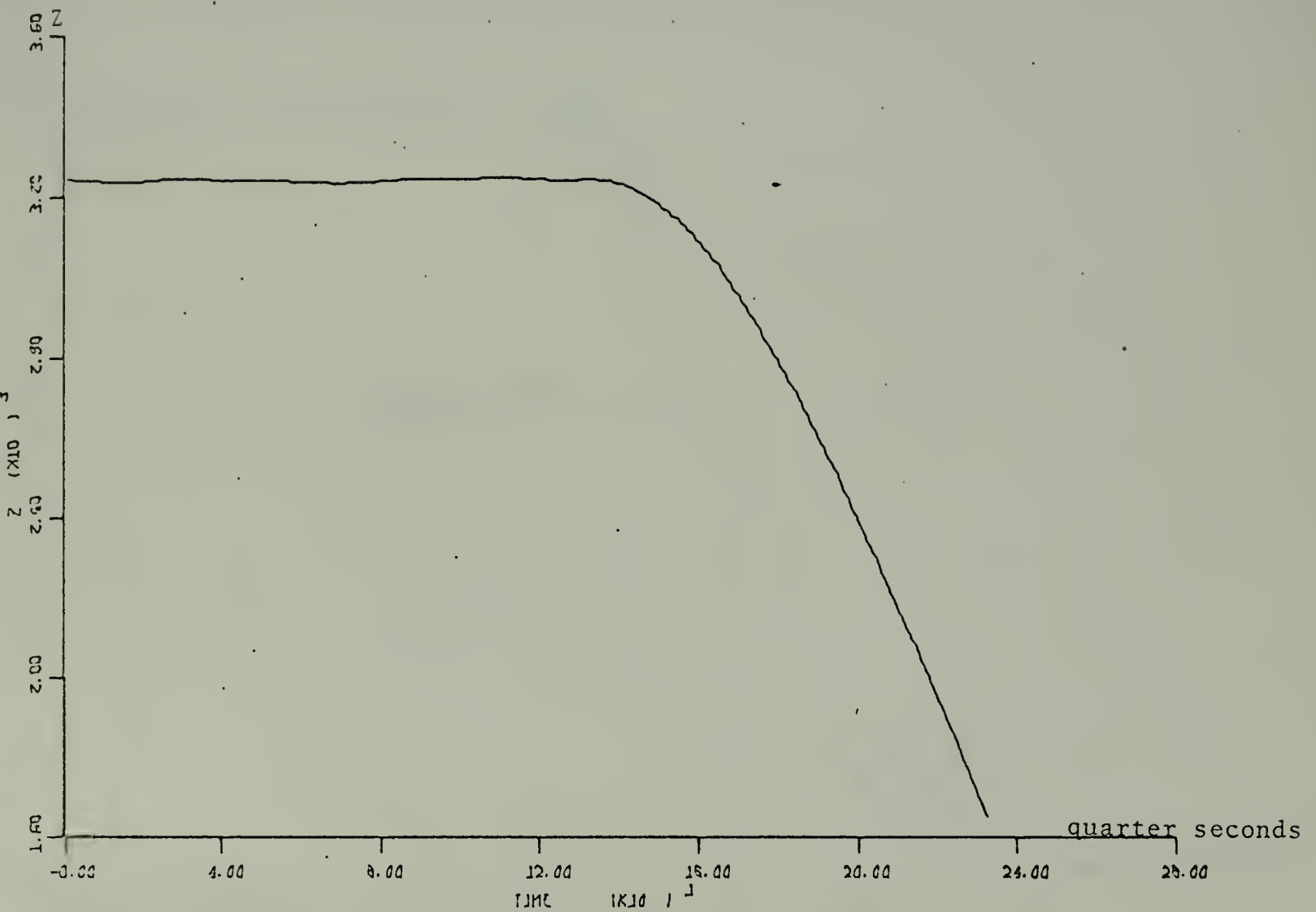

Figure 11. Position estimate by Constant Velocity Model in the Small Q.

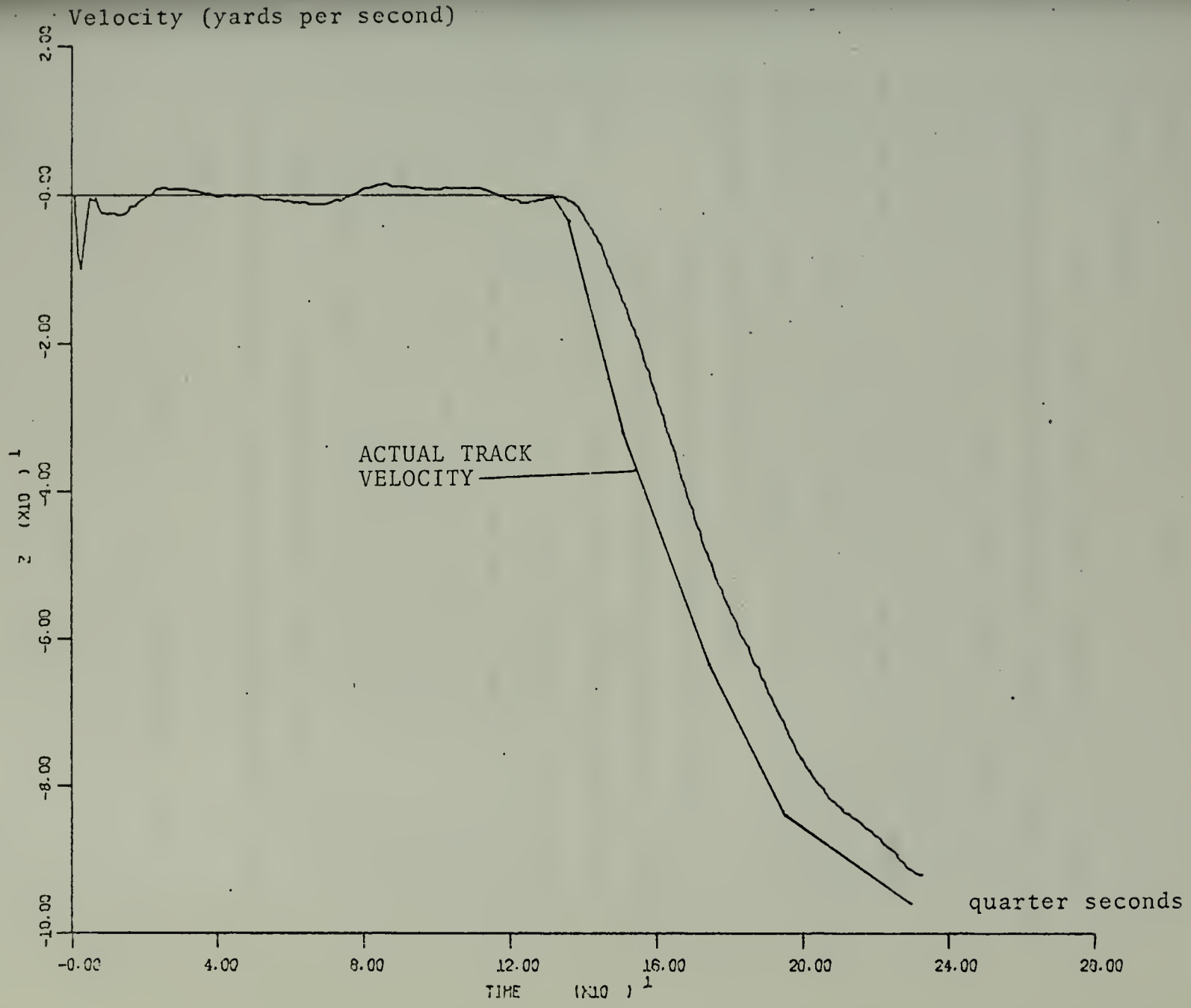

Figure 12. Velocity Estimate by Constant Velocity Model with Small Q.

small Q, but still be able to react to the actual maneuver fairly quickly.

The test results showed that this filter provided excellent position estimates and that the filter did indeed react quickly to the target's dive, as indicated in Figures 13 and 14. It was also found that velocity estimation was relatively inconsistent during the first 128 points and lagged actual target velocity by about 2 yard/sec during the actual dive. In general, however, this filter performed quite well against this track.

c. Constant-Acceleration Model with Small Q

The constant-acceleration plant with a small Q is one of the simplest models used to track accelerated target motion. As with the constant-velocity model with a small Q, the non-zero Q only serves to simplify on-line gain calculations. The steady-state gains in this model should be sufficiently high to track constant-acceleration motion, but the small size of Q means that the filter will be unable to respond to any acceleration rate which may occur during the maneuver and that it should lag behind when the dive is initiated.

It was expected that in general the filter would provide good target estimates of position and velocity throughout the track, but that the filter would be unable to respond accurately if the aircraft did not perform a constant-acceleration dive. Because the Q value was so small, it was further expected that this filter would perform better than the two

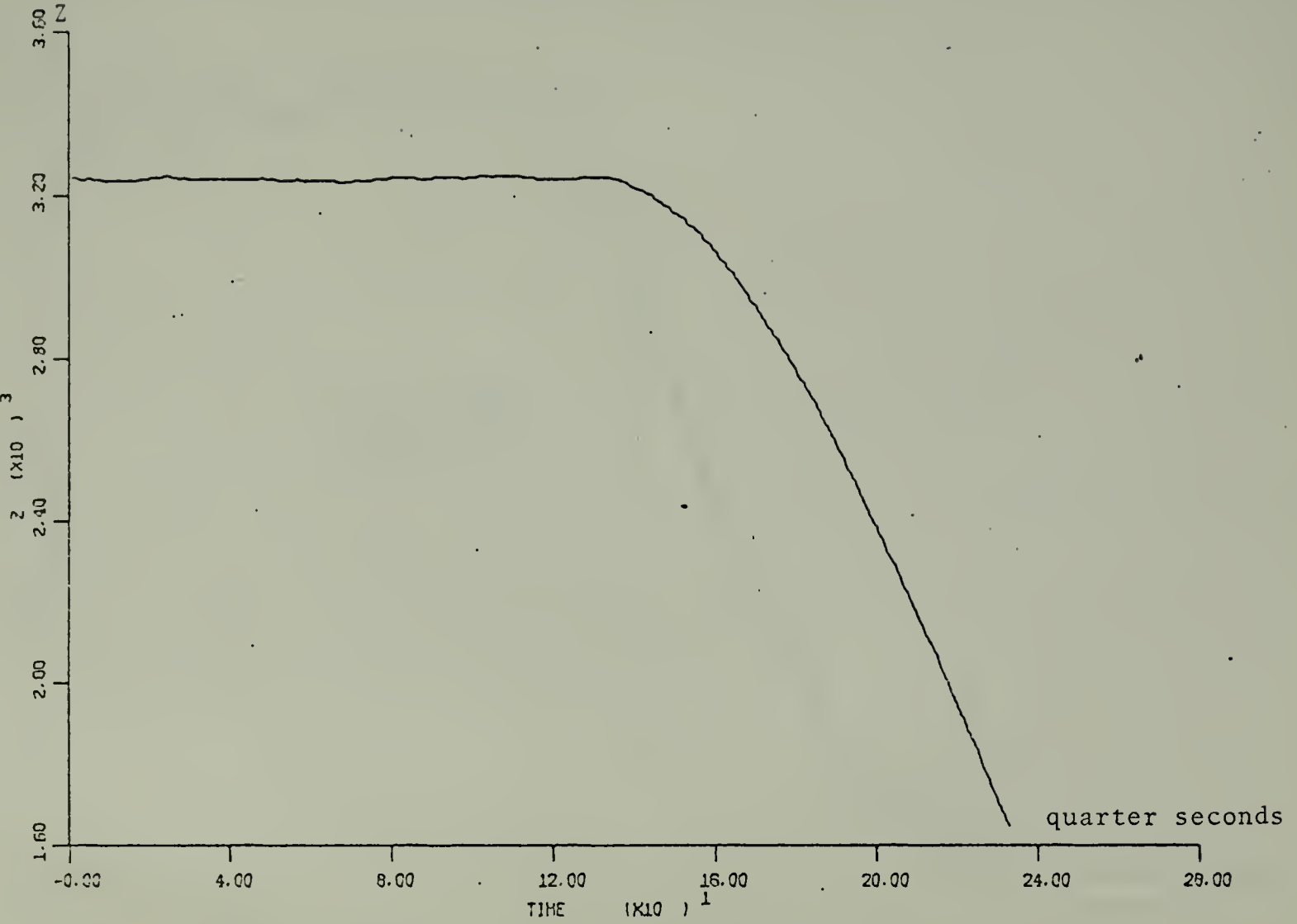

Figure 13. Position Estimate by Constant Velocity Model with Large Q.

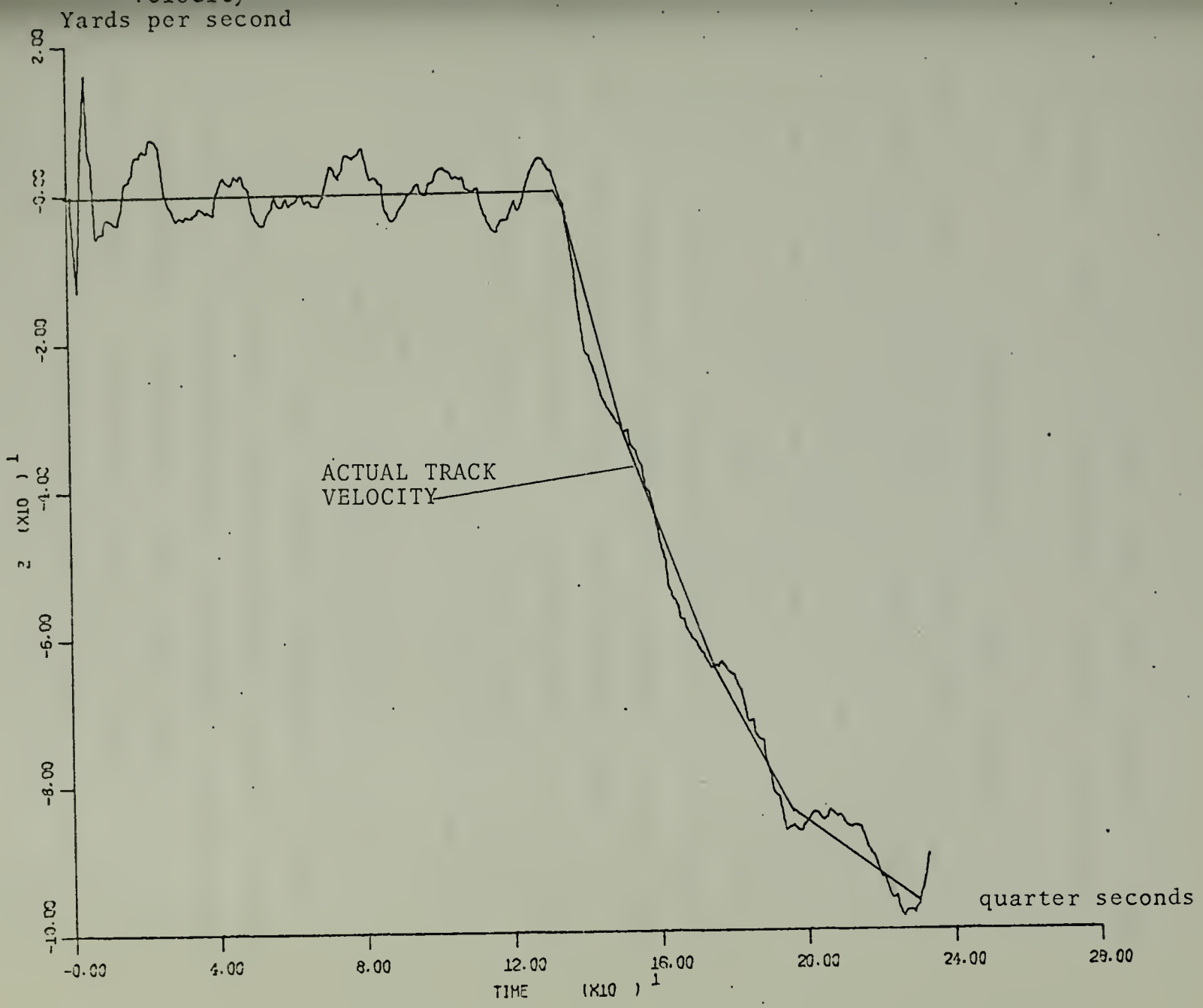

Figure 14. Velocity Estimates by Constant Velocity Model with Large Q.

other third-order filters during the constant velocity portion of the track, but that it may tend to respond to large maneuvers somewhat more slowly than the other third-order filters.

It was found that this filter performed creditably in position and velocity estimates during the constant-velocity portion of the track, as indicated in Figures 15 and 16. However, 14 consecutive position estimation errors between 4 and 10 yards were generated about two or three seconds after the dive began. In addition, velocity estimates appeared to lag somewhat behind the actual velocity at the beginning of the dive. This seemed to indicate that the filter gains had become so small in the steady state that the filter was unable to respond quickly and accurately to the aircraft's maneuver. About two seconds after the dive geban, however, position and velocity estimates once again were excellent.

d. Constant-Acceleration Model With Large Q

The constant-acceleration model with a large Q is designed to provide accurate estimates when an acceleration rate is encountered during a supposedly constant-acceleration maneuver. The optimum filter Q for this track has not been evaluated, so the Q was arbitrarily selected as one-tenth that of the coloring filter's Q. The gain schedule is kept at relatively high values so that the filter should be able to respond effectively to such a maneuver.

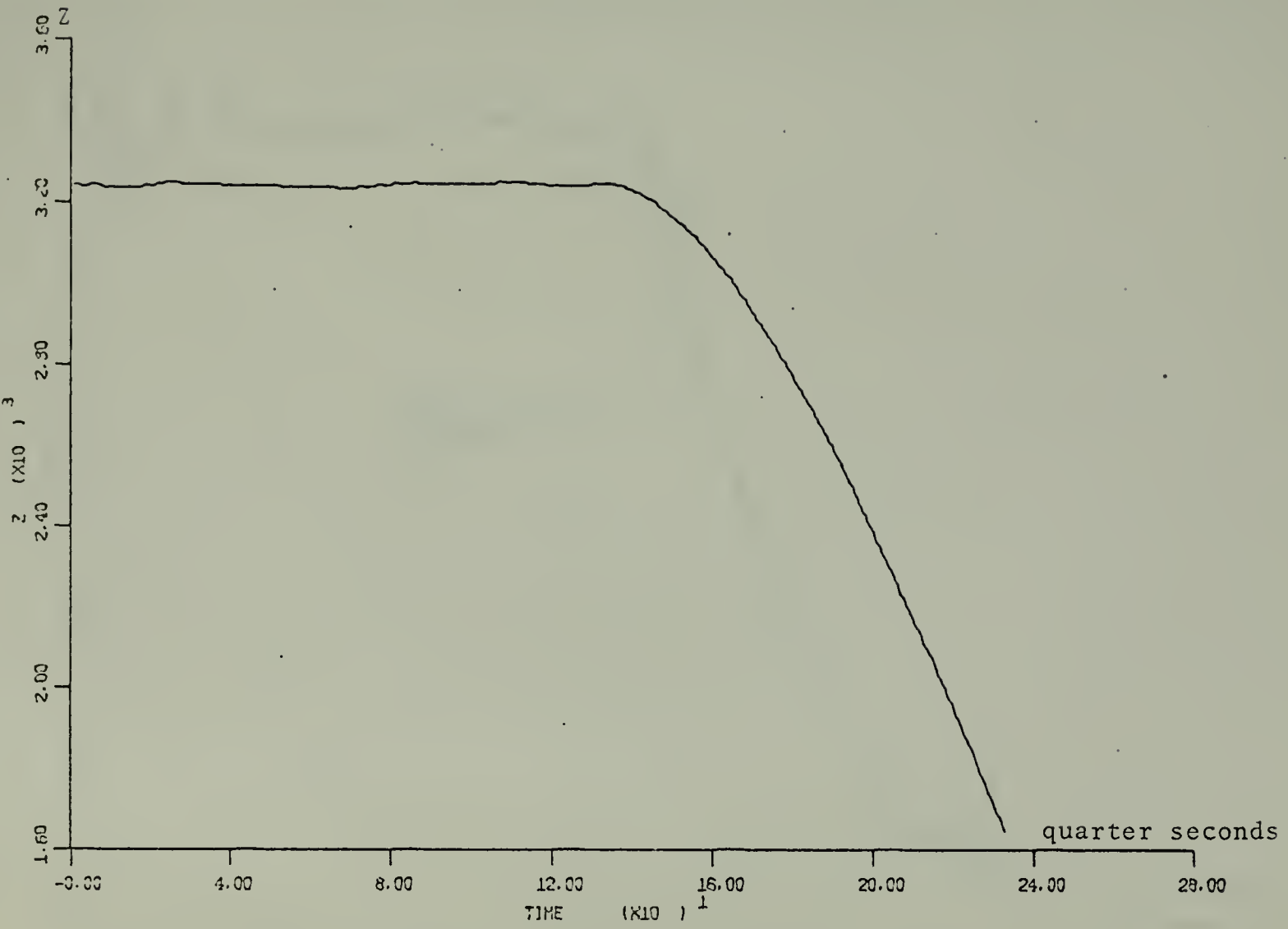

Figure 15. Position Estimate by Constant Acceleration Model with Small Q.

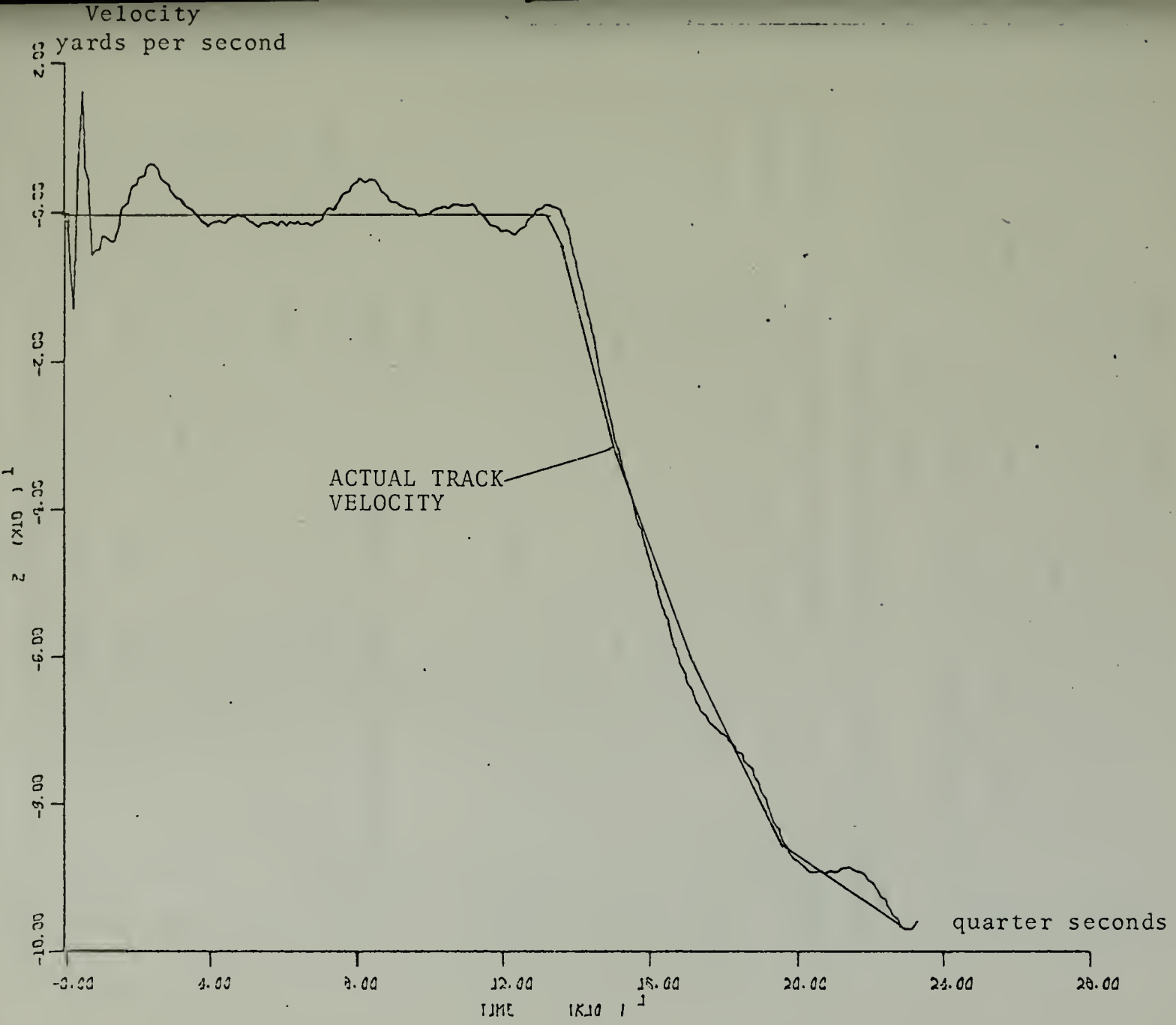

Figure 16. Velocity Estimate by Constant Acceleration Model with Small Q.

Filter performance was expected to be excellent during all portions of the track and was expected to exceed the performance of the $1/s^3$ filter with small Q during the dive. However, the presence of the large Q should provide somewhat more inconsistent estimates during the constant-velocity phase of the track.

The results anticipated were in fact achieved with this filter, as shown in Figures 17 and 18. The mean position estimation error was consistently small and the position estimates were consistently accurate. The velocity estimate did tend to be relatively inconsistent as it oscillated about the true velocity value during the constant-velocity portion of the track. The maneuver was quickly detected and the velocity estimates are very accurate throughout the dive.

e. Coloring Filter

Finally, the constant-velocity-augmented-state-transition-matrix model (coloring filter) was tested against the same GFCS MK86 track. In this model of the plant, the magnitude of the acceleration of the expected maneuver is an important factor in selecting the proper Q, so that the optimum gain schedule will be used. Since the test track was known to contain a ½ g dive, the optimum Q should be that Q with which the coloring filter generated the ½ g dive; this was therefore the number selected for filter testing.

It was expected that this filter would perform about the same as the constant-acceleration model with a

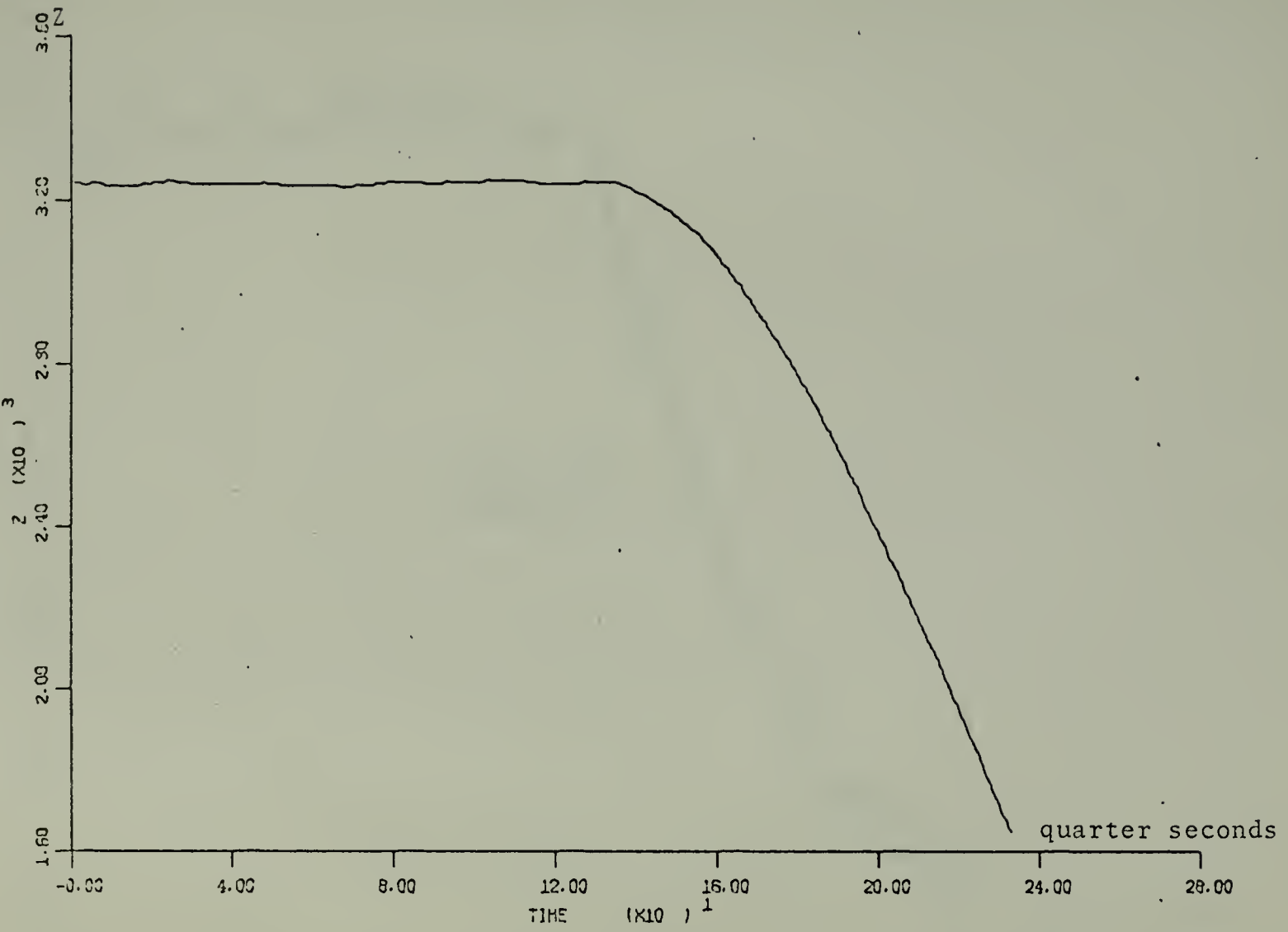

Figure 17. Position Estimate by Constant Acceleration Model with Large Q.

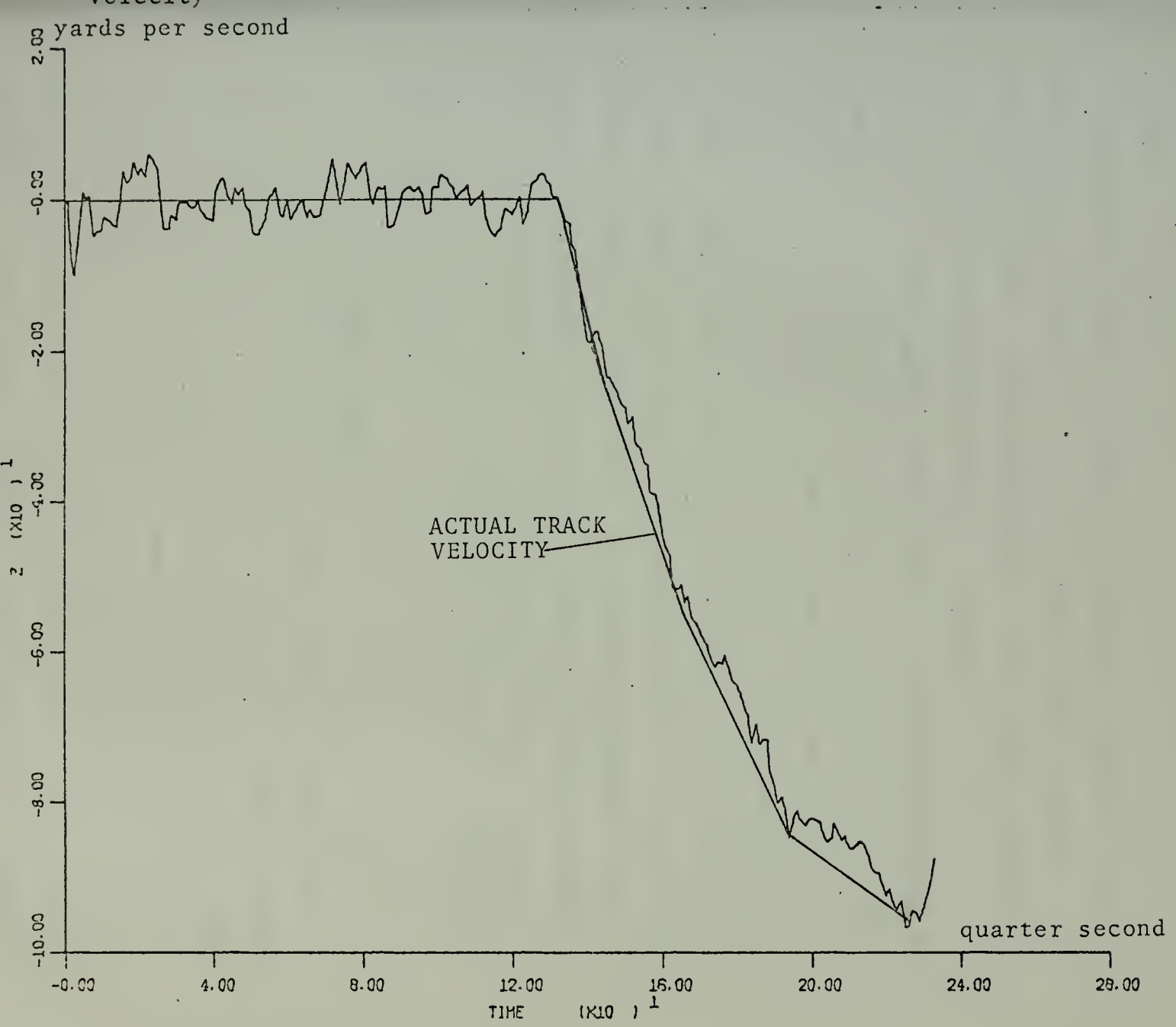

Figure 18. Velocity Estimate by Constant Acceleration Model with Large Q.

large Q. The filter gains should be low enough during the constant velocity portion of the track to allow smooth tracking and provide accurate estimates of position and velocity, yet the size of the Q should allow the gains to be large enough so that the filter reacts quickly and accurately to the maneuver when it occurred.

Once again, the testing in general fulfilled the expectations of filter performance, as can be seen in Figures 19 and 20. The filter tended to show somewhat tighter velocity estimate during the constant velocity phase of the target track than did the previous filter, and velocity estimates during the target dive matched quite well with the actual values of the track. The filter estimated target position accurately, although the mean of position estimation error was about 0.2 yards larger than that of the previous filter. This filter also reacted very quickly to the target maneuver.

3. Test Result Summary

The average filter position estimation error for each filter tested is indicated in Table II. This performance criterion shows that the constant-velocity plant model with a large Q had a smaller mean estimation error on the average than did the other more complicated filters, a somewhat surprising result. Note, however, that there is little difference between the constant-velocity model with augmented state transition matrix and the constant-acceleration model with a large Q.

Figure 19. Position Estimate by Constant-Velocity Augmented State Transition Matrix Model.

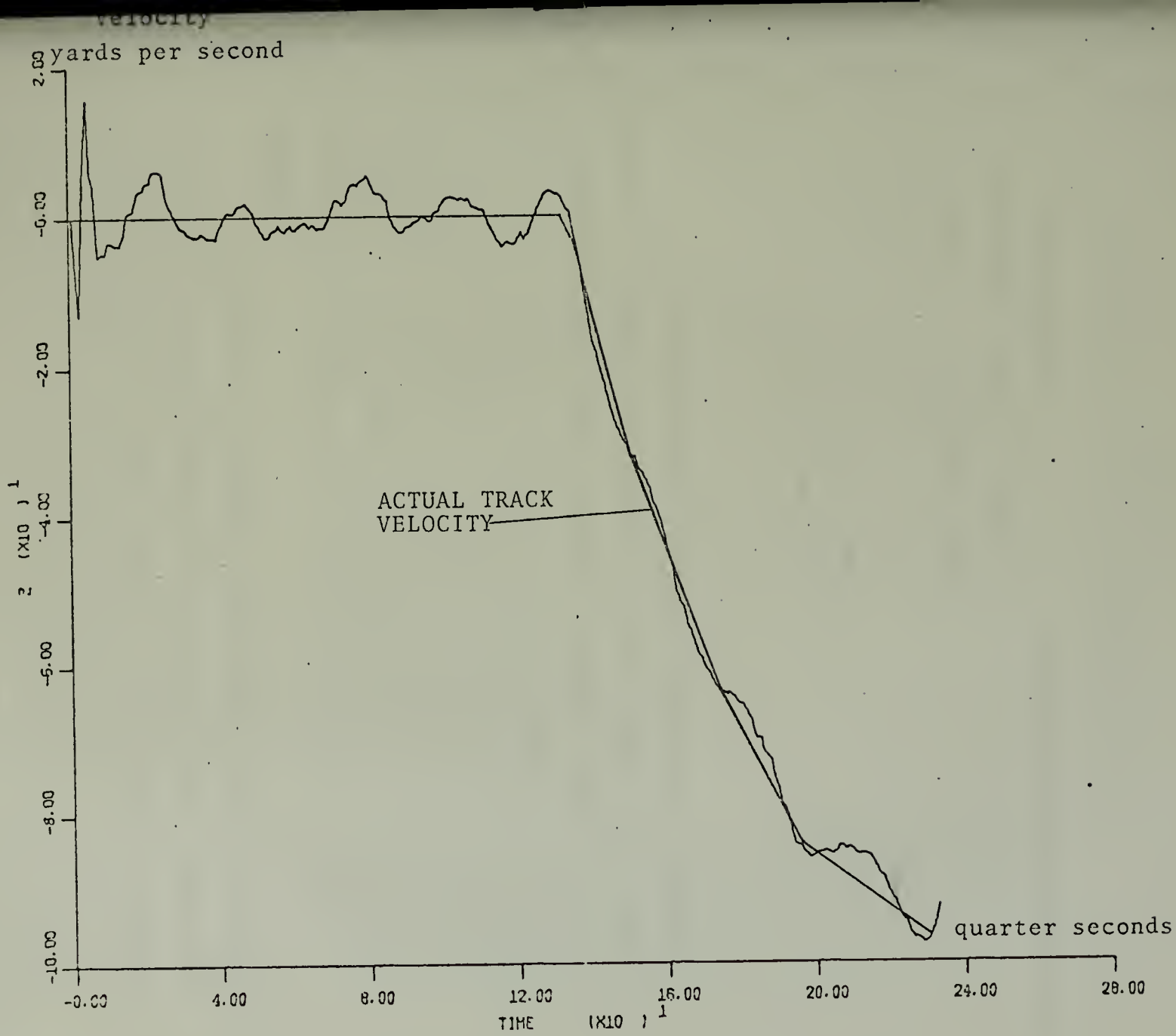

Figure 20. Velocity Estimate by Constant Velocity Augmented State Transition Matrix Model.

Table II.

Average Filter Position Estimation Error

Filter Model	Average Estimation Error(yds)
1. Constant Velocity, Large Q	0.7453
2. Constant Acceleration, Large Q	0.9707
3. Coloring Filter	1.1506
4. Constant Acceleration, Small Q	2.0066
5. Constant Velocity, Small Q	8.3009

For the position estimation performance criterion, it was found that the constant-velocity model with small Q performed better before the dive occurred than did the other four filters. However, the other four filters performed far better than the constant-velocity filter did during the actual maneuver, as should be the case. There did not appear to be any significant difference in position estimation accuracy among these four filters during the dive, however.

The velocity estimate performance criterion seemed to point out the major differences among the five filters, especially during the target maneuver. The constant-velocity model with small Q gave poor estimates during the dive, as was expected; the constant-acceleration model with small Q appeared to lag in velocity by about one yard and two seconds in time when compared to the actual track. The constant-velocity model with large Q tended to lag actual velocities

by about one yard, while the constant acceleration model with large Q and the augmented state transiton matrix model both seemed to give the best estimates of velocity during the dive. All of the last three filters, however, seemed to sense the target dive rather quickly and lagged the initial target maneuver only by one second.

IV. CONCLUSIONS

It has been shown that a coloring filter can be used to generate maneuvering target tracks in one dimension and that the acceleration attained during the maneuver is dependent upon the standard deviation of the white input forcing noise. In particular, it was shown that with certain filter parameters the coloring filter generated a track containing a ½ g dive which was similar to an actual track experienced during the testing of the GFCS MK86.

Within rather restrictive testing conditions, it was also shown that the filter derived from the augmented state equations could be expected to provide accurate and timely position and velocity estimates when used against an actual target track. It must be emphasized, however, that the testing was done in one dimension only using noisy track data with the actual position and velocity of the aircraft not precisely known. Nor is it certain that the noise on the track used was indeed representative of the noise which could be expected since only one run through the Monte Carlo Simulation Program was performed. It must also be concluded that while this filter performed accurately against this track, two other filters performed at least as well on the same track.

Several areas for future investigation suggest themselves. The amount of correlation obtained during the maneuver

simulation using the coloring filter depends directly upon the value chosen for α. For this thesis α was selected as 0.2, which corresponds to a time constant of 5 seconds. It may be that a different value for α would model maneuvers more effectively.

Some scheme for adapting the Q of the filter to changing conditions could also be investigated. Since a single Q must be chosen in advance, it essentially represents the size of the expected maneuver. Greater efficiency could be obtained if some method could be devised which would decrease the magnitude of Q (thereby decreasing the gains) for slow or non-maneuvering targets, and increase Q (thereby increasing the gains) when larger maneuvers are detected.

It was previously noted that the filter was tested under very restrictive conditions; a final area for investigation is therefore in testing the filter using Monte Carlo simulation. Since the filter testing was performed only in one-dimension using a noisy track of a ½ g maneuvering target with the true position, velocity and accelerations unknown, a Monte Carlo simulation could be conducted which would give a more realistic test of the filter's ability to estimate target position and velocity. Such a simulation should include multi-dimensional tracks with radically maneuvering targets whose position, velocity and accelerations are precisely known. In this manner it may be possible to better discriminate among the three filters which gave comparable results.

APPENDIX A

RELATIONSHIP BETWEEN WHITE AND COLORED NOISE STANDARD DEVIATION

Given the discrete equation

$$x(k+1) = \Phi x(k) + \Delta w(k).$$

With the assumption that $x(k)$ and $w(k)$ are independent and

$$x(o) = 0,\ E[w(k)] = 0,\ E[w^2(k)] = \sigma^2,\ E[x(k)] = 0 \text{ for all } k$$

where σ is the standard deviation of the white input noise.

Then

$$\begin{aligned} E[x^2(k+1)] &= E[\Phi^2 x^2(k) + 2\Phi\Delta x(k) + \Delta^2 w^2(k)] \\ &= \Phi^2 E[x^2(k)] + \Delta^2 E[w^2(k)] \\ &= \Phi^2 E[x^2(k)] + \Delta^2\sigma^2 \end{aligned}$$

Let $P(k) = E[x^2(k)]$ and $P(o) = 0$

Then

$$P(1) = \Delta^2\sigma^2$$

$$P(2) = \Phi^2[\Delta^2\sigma^2] + \Delta^2\sigma^2$$

$$\vdots$$

$$P(n) = \Delta^2\sigma^2[\Phi^{2n} + \Phi^{2(n-1)} + \cdots + \Phi^2 + 1].$$

Summing to infinity,

$$P(\infty) = \sigma^2\frac{\Delta^2}{1-\Phi^2} \quad (1)$$

For the characteristics of the coloring filter of $\alpha = 0.2$ and $T = 0.25$,

$$P(\infty) = .02564\sigma^2$$

so that in steady state the standard deviation of the colored noise is .1601 that of the white forcing noise.

BIBLIOGRAPHY

1. Aldrich, G. T. and Krabill, W. B., "An Application of Kalman Techniques to Aircraft and Missile Radar Tracking," AIAA Journal, July 1973, pp. 932-938.

2. Ketron, M., MSEE Thesis, Naval Postgraduate School, Monterey, California, June 1974.

3. Singer, R. A. and Behnke, K. W., "Real-Time Tracking Filter Evaluation and Selection for Tactical Applications," IEEETransactions on Aerospace and Electronic Systems, January 1971, pp. 100-110.

4. Sorenson, H. W., "Kalman Filtering Techniques," Advances in Control Systems, Academic Press, Vol. 3, pp. 219-254.

INITIAL DISTRIBUTION LIST

		No. Copies
1.	Defense Documentation Center Cameron Station Alexandria, Virginia 22314	2
2.	Library, Code 0212 Naval Postgraduate School Monterey, California 93940	2
3.	Professor D.E. Kirk Department of Electrical Engineering Naval Postgraduate School Monterey, California 93940	1
4.	LCDR David Howard McKinley USN Box 285 Malabar, Florida	1
5.	Professor H.A. Titus Department of Electrical Engineering Naval Postgraduate School Monterey, California 93940	1
6.	Professor J.R. Ward Department of Electrical Engineering Naval Postgraduate School Monterey, California 93940	1
7.	LT. D.F. Regener, USN Naval Ship Missile System Engineering Station Space City 8 Port Hueneme, California 93043	2

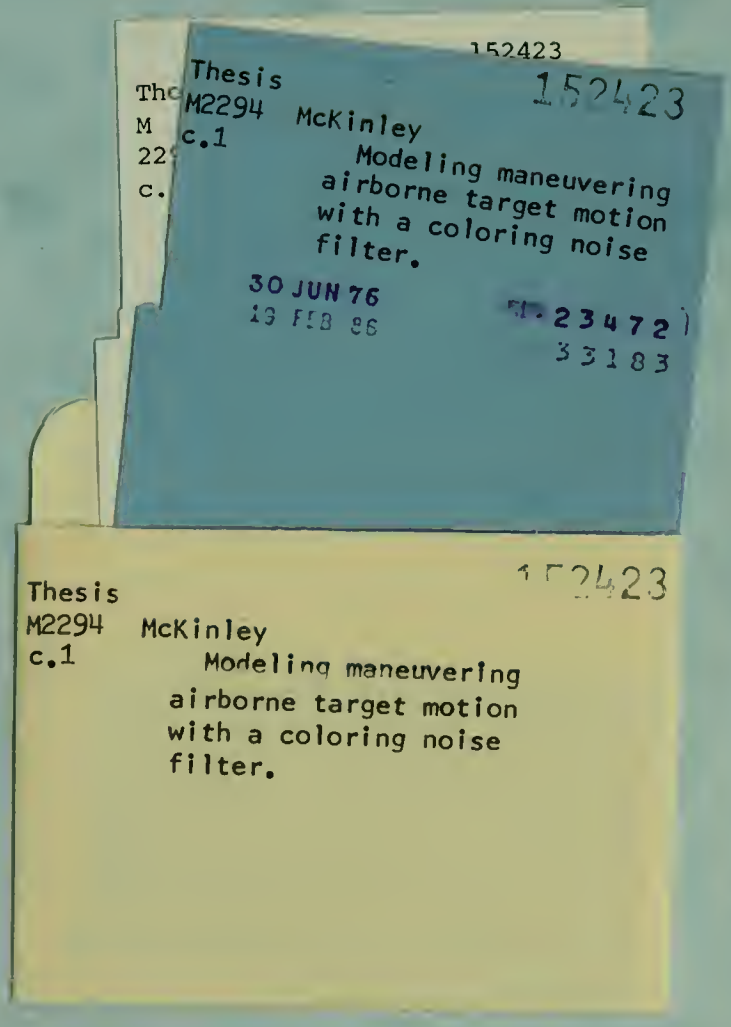

152423
Thesis
M2294 McKinley
c.1 Modeling maneuvering airborne target motion with a coloring noise filter.